MONITEQ

Monitoring Environmental Quality
Moniteq Ltd., 2 Silver Avenue, Toronto, Ontario, Canada M6R 3A2 (416) 533-2381 Telex 06-22847

A DEMONSTRATION OF THE FEASIBILITY OF USING REMOTE SENSORS TO MEASURE SPECIFIC SO_2 SOURCE EMISSIONS

PREPARED BY
MONITEQ LTD.
2 SILVER AVENUE
TORONTO, ONTARIO

Fisheries and Environment Canada | Pêches et Environnement Canada

THIS REPORT WAS PREPARED
FOR ENVIRONMENT CANADA BY
MONITEQ LTD. UNDER DEPT.
OF SUPPLY & SERVICES
CONTRACT NO. OSS77-00215

January, 1979
MTR 78-9

S. C. Jain, Ph.D., P.Eng.
T. V. Ward, Ph.D.
S. Onlock, B.A.

TABLE OF CONTENTS

LIST OF FIGURES

8.18 Comparison of Hydro Mass Balance Data to Mass Flux Calculations Using Meteorological Data from Tethersonde

8.19 Comparison of Hydro Mass Balance Data to Mass Flux Calculations Using Meteorological Data from a Vector Average of Pibal Data (Averaged 100 - 500m)

8.20 Resolution of Calculated Mass Flux from Individual Stacks, March 24, 1978

8.21 Resolution of Calculated Mass Flux from Individual Stacks, March 29, 1978

8.22 Histograms of Differences Between Hydro Mass Balance Data and Calculated Mass Flux. Upper Histogram Uses Sampling at 20% while Lower Samples at 10%.

LIST OF TABLES

ACKNOWLEDGEMENTS

MONITEQ wishes to express their appreciation for the opportunity to participate jointly with both the Canadian Department of Fisheries and Environment and the Ontario Ministry of Environment in undertaking this evaluation of the potential routine operational applications of commercially available remote sensors, and for their continuing support of the field evaluation and use of these sensors in the separation of multi-source emissions, international boundary flows, and long range transport of air pollutants.

In particular, MONITEQ expresses their gratitude to the following individuals whose time, effort and support prior to and during this project were instrumental in fulfilling the original objectives:

Dr. T. R. Ingraham, Director, Technology Development Branch, APCD, EPS and his staff; Mr. M. J. Bumbaco, Surveillance Branch, EPS, Scientific Authority; Dr. S. Stevens, Air Resources Branch, MOE, and his staff, in particular, Dr. G. Van Volkenburgh; Mr. D. K. A. Gillies, Manager, Environmental Protection, Ontario Hydro and his staff, in particular, Ms. J. R. Ryan; and Mr. M. J. Northfield and Mr. D. McLeod of the Nanticoke Generating Station. Suggestions and helpful discussions with Dr. M. M. Millan, AES, are also gratefully acknowledged.

1. INTRODUCTION AND GENERAL BACKGROUND

1.1 MAJOR OBJECTIVES

Over the past several years, a considerable amount of work has been carried out in Europe and North America on the evaluation of remote sensing techniques as a tool for monitoring atmospheric pollution (see Appendix). Remote monitoring of gaseous pollutants can be successfully applied in the study of long range transport of pollutants, evaluation of horizontal dispersion coefficients, and wind shear effects, photochemistry of conversion processes and deposition from pollutant plumes, source identification and separation, and source emission monitoring and mass flux calculations. Remote sensing methods have also aided in development and verification of predictive atmospheric models.

The application of remote sensing techniques which has, perhaps, its greatest practical impact, is in source emission monitoring of SO_2, where the mass flux measurement of sulphur dioxide is made remote from the source and is related back to the source strength. Current techniques for source emission monitoring of stacks not instrumented for pollution control, are by material balance or extractive sampling. Stacks which are instrumented have either in-situ point monitors, automatic extractive monitors, or long path, across-the-stack optical monitors where the measurement is the integrated burden of the specific gas of interest. Extractive and in-situ point sampling suffer from effects due to local inhomogenities, stratifications and perturbations within the flow, and from the difficulty in ensuring integrity of the sample from the time it is collected until it is analyzed. The long path electro-optical devices, on the other hand, provide information most representative of the nature of total pollutant flow; however, they suffer from the difficulty of operating in a very harsh environment.

Outside an emitter's property, remote sensing techniques provide integrated burdens of pollutant gas above the sensor by simple interpretation of the measurements made with electro-optical devices. This aids in identification, separation and quantization of emissions of a principal offending polluter from an area or multiple sources. To achieve the same identification with ground level point sampling is difficult. Remote sensing techniques provide a good quality of useful data and are not limited by the difficulties encountered by either in-stack sampling or ground level ambient monitors.

With proven electro-optical remote sensing techniques, it is possible to mobilize immediately with available sensors to the area of concern and sufficient measurements can be made within one to two hours (within meteorological constraints). With the use of experienced field personnel, and with the use of a correct interpretation methodology, it is possible to provide reliable results for air quality decision-making within a short period of time. Remote sensing methods also offer greatly reduced costs and personnel requirements, and yield reliable, meaningful data. The technique has the potential of providing 24-hour coverage with minimal weather restrictions.

The purpose of this study was to demonstrate the operational feasibility, and to develop the methodology of measurement of source emissions of sulphur dioxide, as a routine and cost effective method, by using commercially available remote sensing instruments. It was also intended to obtain supporting data to determine the advantages and to define the operational limitations of the remote sensing method. Potential application of an infrared sensor to extend the capability to 24-hour measurement was also planned to be studied.

To obtain data for this study, a sulphur dioxide source was selected in the village of Nanticoke, Ontario. The thermal generating station operated by Ontario Hydro offered a unique location because of the interest of various Government agencies and industry in the general

air quality of the area in anticipation of its planned industrial expansion. Corroborative mass emission data are obtained by Ontario Hydro engineers on an hourly average basis from mass balance, with measurements of the fuel consumption, sulphur content of fuel, and excess air. Ontario Hydro meteorological and environmental scientists also obtain meteorological data on a routine basis from a tower located at about 12 km from the source in Jarvis, Ontario. These data were made available to MONITEQ and comparison of these routinely collected data with the data obtained during this field program has been carried out.

During this study, remote sensing data were obtained to measure source emissions from the two stacks of the generating station. Emissions from the two separated stacks, as well as their combined totals, were obtained whenever resolution of the two plumes was possible. In all cases, the source emission from the entire plant was computed and compared with the sulphur mass balance computations of the separated or merged plumes.

The meteorological data required to interpret the correlation spectrometer measurements were obtained with the double theodolite balloon tracking system, the minisonde system, and with the tethersonde system. These data were compared with those from the instrumented meteorological tower at Jarvis. Recommendations are made in this study regarding how to make the meteorological measurements cost effective, less cumbersome, and more reliable.

The study was carried out in three distinct phases. Firstly, a literature review was performed to evaluate the results and methodology used in earlier remote sensing studies. Secondly, meteorological and environmental data were collected in the field. Data from six different days taken during a 13-day period are presented and evaluated in this report. Thirdly, data analysis and interpretation was carried out to carefully interpret the measurements and assess the feasibility of this methodology.

1.2 THE FIELD PROGRAM

Weather conditions permitted reliable data collection on six days only, during the period of 20th March to 1st April, due to the unusual amount of rain, snow and fog on seven days during this period. Data collection methodology is described in Chapter 6.

During two days, it was possible to obtain the mass flux of sulphur dioxide emitted from each single individual stack. The mass flux for the combination of the two stacks was computed for all collected data. Field evaluation, data evaluation and analysis was also carried out for the different meteorological systems involved.

A complete description of methods used to extract and interpret the remote sensing and meteorological data is presented in Chapter 7. Correlation spectrometer data were transferred to computer compatible tapes and were analyzed with a DecSystem-10 timesharing system with the use of a Xerox of Canada Diablo-1641 computer terminal. The meteorological data were also transferred into the computer and software developed to analyze the data.

In this program, the results of the remote sensing method are compared with the results of the mass balance technique used by Ontario Hydro. In order to use the remote sensing method as a compliance method, it should, ideally, be compared against a reference method, so that definitive confidence levels may be determined. However, in the absence of the reference method, this study yields relatively high confidence when compared to the mass balance method, and may be used for identification of sources requiring full compliance tests.

When this study was initially planned, it was intended to compare the remote sensing method to a standard method. However, because of the immediate interest in the area of Nanticoke, the Ontario Hydro location was selected in consultation with the interested government organizations.

2. SUMMARY

A successful field program has been carried out during extreme winter weather conditions in March, 1978, on the northern shore of Lake Erie, when SO_2 emissions from the Ontario Hydro Thermal Generating Station at Nanticoke were monitored with remote sensors, and measurements compared with mass balance data provided by the utility.

The primary objectives of this study were:

1) to define the confidence levels, operational and meteorological limitations of using perimeter surveying remote sensing as a routine operational tool to obtain source emission data;
2) to evaluate two different techniques for collecting wind speed and direction data at or close to the survey location, and compare these data with that obtained from an instrumented meteorological tower in the vicinity ($\sim$ 12 km) of the source.

A secondary objective of this study was to evaluate the capability of an experimental infrared remote sensor to operate in a similar configuration to the commercially available correlation spectrometer operating in the ultraviolet, and, if possible, to extend its operation to 24-hour coverage.

3. CONCLUSIONS

The results of this study show that, within a radius of up to 2.5 km from the Nanticoke Generating Station, 86% of the total remotely sensed SO_2 source emission measurements made on six days over a 13-day period in March, 1978, were within $\pm$ 25% of the hourly average mass balance data provided by Ontario Hydro.

Specifically, the mass emission data collected remotely on each of 21 separate sampling periods of from 30 to 60 minutes' duration, had a relative accuracy of $\pm$ 25% when compared to the hourly mass balance data.

The confidence levels reported here assume a negligible error in the hourly mass balance data; however, analysis of the sulphur content of the fuel on two occasions over the period of the study was found to vary by 5%. This is a lower limit on the accuracy of material balance under these conditions.

The consistency of the run-to-run data taken during each of the 21 discrete sampling periods (30 - 60 minutes) as determined from the standard deviation, shows that in 95% of the total data collected, the run-to-run variation is within $\pm$ 23%.

Under favourable wind direction conditions, when surveys were carried out parallel to a line joining the two stacks, it was possible to resolve the contribution of each stack to the total source emission within the above confidence levels.

The only previously reported data* required at least eleven 20-minute sample periods; i. e., a minimum of four hours of data, to achieve

*Evaluation of the Correlation Spectrometer as an area SO_2 Monitor. EPA report # 600/2-75-077, October, 1975.

similar confidence levels (in this instance, the difference between remote measurements and EPA Method 6). Our results show that a single sample period of 30 - 60 minutes is sufficient.

The location of the generating station and its internal road network, coupled with the availability of perimeter roads outside the station and flat topography of the local terrain, presented an ideal operational location. Measurement periods of up to nine hours per day were utilized during the study. The only limiting meteorological constraints which occurred during these remote sensing measurements, were those of snow, freezing rain and fog. Under all other meteorological conditions, it was possible to collect data during a 9-hour daylight period.

The evaluation of the wind speed and direction data from both the continuously reading tethersonde and the instantaneous double theodolite pilot balloon measurements at approximately the same location, produced data which was within $\pm$ 12%, standard deviation.

The advantages of the tethersonde are the continuous data produced at the plume height and its unattended operation once launched. These outweigh the use of pilot balloons with half-hourly instantaneous measurements, requiring at least two personnel, on a continuous basis. The major restrictions on the tethersonde system are its upper measurement limitation of 12 to 15 ms^{-1} and the potential difficulty of flying it in a restricted or built-up area.

Comparison of the Pibal and Tethersonde meteorological data with that of an instrumented tower $\sim$12 km from the survey location, shows that, while the wind direction correlates extremely well, the wind speed data taken at the 85-metre height station of the tower was consistently lower by $\sim$ 100% on all occasions, independent of wind direction, and, therefore, could not be used to make source emission measurements. A calibration error is suspected because the wind speed at the 32 m level at the same station is generally higher than the 85 m measurement. Ontario Hydro scientists are re-evaluating the reliability of these data.

The field evaluation of the gas cell correlation spectrometer operating in the infrared proved disappointing, due to signal interferences arising from polarization of the collected radiation with changing orientation with respect to solar elevation. While the data were collected throughout the study, no meaningful interpretation could be achieved without major modifications to the instrument's optical configuration.

4. RECOMMENDATIONS

The results of this study demonstrate the feasibility of using remotely collected SO_2 mass burden data in conjunction with wind speed and direction data obtained from a tethersonde system flown at the plume altitude, and close to the survey location, to provide reliable source emission data on a routine basis under extreme meteorological conditions (Southern Ontario winter).

The following advantages apply to the operation of commercially available remote sensors for routine, relatively accurate and reliable SO_2 source emission measurements:

1) Cost-effective source emission monitoring with one instrumented vehicle; e. g., station wagon.
2) Collection of sufficient data within a short period of time (30 - 60 minutes), when operated within radius of 2.5 km of source.
3) Rapid mobilization and flexibility for routine operations.
4) Non-interference with plant operation.
5) Capable of distinguishing competing sources--and possibly quantifying separate nearby emitters.
6) Effective surveillance monitoring of suspected violations, and air pollution episodes.

Major disadvantages of the technique and limitation of its application lies with adverse weather conditions such as fog, rain or snow. Unavailability of a good network of perimeter roads may present a limitation in specific locations, although it is anticipated that, in most cases, a good road network around a plant will be available. In such cases, airborne measurements can be made using either helicopter or fixed-wing platforms.

Based on this study, the following recommendations are made:

1) An operational survey should be carried out on a source other than a utility and where varying loads will occur, and preferably where continuous in-stack reference methods are available for comparison.
2) A survey should be carried out on a utility over at least two seasons, and preferably four, to demonstrate the capability of year-round monitoring operation under varying loads.
3) Carry out a comparison of the Ontario Hydro mass balance method with standard reference methods in order to relate this study to generally accepted reference measurements.
4) Carry out a perimeter study within 2 - 5 km on multiple sources to attempt to separate and quantify specific sources.
5) Future work should emphasize the need to quantify data in the medium field, > 5 km radius, and relate this data to atmospheric and meteorological parameters; e. g., visibility, radiative transfer, wind speed and direction averaged through the plume. This work should be carried out in order to determine the reliability of extending this technique to the quantification of long range transport.
6) Determine points of impingement of invisible plumes, and track centre line to assist in location of ground level monitoring stations.
7) Investigate the possibility of monitoring low level fugitive emissions either passively or using fixed long path measurements.
8) Analyze historical correlation spectrometer data taken at other locations for its relative accuracy.
9) Carry out further evaluation of the Infrared Gas Cell Correlation technique with its potential for the detection of different pollutants and 24-hour coverage:
   a) look into the possibility of reducing polarization effects due to telescope/sky orientation with the present IR system;
   b) alternatively develop a simple IR system based on the experimental work to date, which will utilize a different optical configuration to reduce interfering polarization effects.

5. INSTRUMENTATION AND CALIBRATION

5.1 CORRELATION SPECTROMETER

5.1.1 Instrumentation and Design

The correlation spectrometer (Millan et al., 1970, Moffat and Millan, 1971), operating on the Beer Lambert law of absorption, is designed to measure the quantity of a specific gas (in this instance, SO_2) present in the line of sight from a suitable source of electro-magnetic radiation by displaying the dispersed spectrum of the incoming radiation at the exit mask. Using scattered solar radiation as the source, the absorption signature of SO_2 in the instrument line of sight is dispersed within the grating spectrometer and displayed at the exit mask. The circular mask, which is divided into four segments, is designed to allow alignment to specific features within the SO_2 absorption band. Adjacent segments are designed to pass absorption maxima and minima and by rotation of the mask, a modulated signal is produced on the photomultiplier tube. The modulated signal is processed to provide an output proportional to the concentration path length product of SO_2 in the path.

5.1.2 Calibration

The correlation spectrometer includes two internal cells containing SO_2. These cells can be manually inserted in the optical path to provide a suitable calibration of the instrument.

In addition, for this study, a full absorption curve of growth was carried out in the laboratory. It was done to verify these internal values prior to the field program and hence, ensure reliable quantitative data over the anticipated range of the measurement. Two additional cells containing different burdens of SO_2 were also employed in the field to make calibration measurements in the range of interest.

The output in volts of the instrument is directly proportional to concentration times path length (ppm-metres). The internal calibration cells are initially filled to a known burden at 293°K. These values, in addition to the external cells, were verified during a dynamic calibration using a standard reference source and a one-metre absorption cell.

Curve fitting to the actual response was performed to interpolate and extrapolate experimental readings on the basis of the calibration signals. This was done to account for a non-linear relationship, due to the exponential nature of the absorption law, between instrument output in volts and ppm-m. The units of ppm-m were converted to kg/m^2 by using the relation:

$$
\begin{aligned}
&1 \text{ ppm (at } 293^{\circ}K, 760 \text{ mm Hg)} \\
= \quad &\frac{\text{Molecular wt. of } SO_2}{22.4 \text{ litres}} \times \frac{273}{293} \times 10^{-6} \\
= \quad &\frac{64 \times 10^{-3}}{22.4 \times 10} = 3 \times \frac{273}{293} \times 10^{-6} \text{ kg/m}^3 \\
= \quad &2.66 \times 10^{-6} \text{ kg/m}^3
\end{aligned}
$$

where 293° Kis the temperature at which the internal calibration of the cells was performed. Changes in SO_2 absorption cross section with temperature have a second order effect as the plume is assumed to have equilibrated with background temperature at the measurement location.

5.2 GAS CELL SPECTROMETER

5.2.1 Gas Cell Spectrometer Instrumentation

The infrared gas cell correlation spectrometer (Ward and Zwick, 1975), viewing vertically upwards, detects and modulates the emission signature of SO_2 at its equilibrium temperature (~273°K) when viewed against a cold sky (~240°K) background. This signature is passed to the two arms of the instrument, which, in the absence of SO_2, have been forced to a balanced condition while viewing the cold sky. At the detector from the arm containing the sample cell of SO_2, no signal is detected. At the

detector in the arm containing the sample cell of N_2, there is an increase in signal due to emissions from the SO_2 target gas. This difference signal is processed to obtain an output proportional to the concentration times path length of SO_2 in the path at the SO_2 equilibrium temperature.

5.2.2 Gas Cell Spectrometer Calibration

Prior to field operation, the Gas Cell Spectrometer was calibrated in the laboratory using a commercial black body with a one-foot-square aperture as the background source. Due to the undesirability of using SO_2 in a windowless cell, the spectrometer was calibrated only in absorption. This absorption measurement was then inverted to give a corresponding emission calibration. 10 cm diameter gas cells with 4.0 mil transmitting mylar windows were charged with varying concentrations of SO_2 and placed between the spectrometer and the black body source. Minimum detectable signal levels with a signal to noise (peak to peak) of one and a one-second time constant were found to be $\sim$ 500 ppm-M, SO_2 in emission.

5.3 TETHERSONDE

The tethersonde system consists of a lightweight instrument package suspended from a tethered balloon. The system can operate up to an altitude of 800 m and is easily operated by one person. The instrument package measures dry bulb temperature (thermistor), wet bulb temperature (wick covered thermistor), pressure (aneroid capsule), wind speed (cup anemometer) and wind direction (balloon and magnetic compass) and transmits their values via an F.M. transmitter at 403 MHz. The time multiplexed data are received and recorded in the base van with three measurements occurring each minute. Calibration checks on the wind speed, temperature, and wind direction were carried out and were found to meet or exceed those listed by the manufacturer. Height of the tethersonde was obtained from the pressure measurement.

Signal Ranges	1) Temperature	$25^{o}C$ with accuracy of $0.5^{o}C$ (-30^{o} to $+45^{o}$ in 6 different ranges of 25^{o} set by a DIP switch)
	2) Pressure	0 to 100 mb $\pm$ 1 mb
	3) Wind Speed	0.5 to 10 m/sec $\pm$ 0.25 m/sec
	4) Wind Direction	0 to 360^{o} from North $\pm$ 5^{o}

5.4 THE PILOT BALLOON SYSTEM

The vertical profiles of wind speed, wind direction, and temperature were provided by tracking pilot balloons with two theodolites. The temperature information was obtained by attaching a minisonde to the balloons. Measurements of elevation and azimuth of balloon with respect to a baseline were used to determine the exact position of the balloon at intervals of 30 seconds. It will be discussed in Chapter 7 that only three of the four elevation and azimuth readings are required to determine the position of the balloon and the fourth reading can be used to determine the reliability of the data. Prior to the study, both of the theodolites were aligned. The theodolites used in this study measured both elevation and azimuth angles with the help of a screw calliper with an accuracy of 0.05^{o}.

5.5 MINISONDE SYSTEM

The minisondes were used in conjunction with the pilot balloons to provide a temperature vs. height profile. The sonde consists of a lightweight package containing a thermistor and an F.M. transmitter powered by a 9V transistor battery. The F.M. signal (at 403 MHz) is received and recorded in the base van. The ground temperature was measured with a calibrated thermistor and the temperature difference between temperature at a particular height and the ground was computed by using the sensitivity quoted by the manufacturer. The manufacturer's calibrations were checked, and found to be within the claimed error.

5.6 DATA ACQUISITION SYSTEM

In the past, the correlation spectrometer data have been recorded on chart records, and hand-digitizers have been used prior to analysis on digital computers. In this study, a microprocessor-based data acquisition system built by MONITEQ was employed to record the data digitally in the field.

Briefly, the output voltage of the spectrometer is digitized through an A/D converter and one reading per second is recorded as 22 characters on a cassette tape recorder. In addition to the spectrometer response, actual time and odometer readings are also recorded each second. The data are formatted as sequential ASCII characters and recorded at 300 baud rate. Data from each one-second interval are separated by a line feed and carriage return.

These data can be played back in similar fashion, and can be accessed by a large scale digital computer facility. Recording of the data in digital form in the field eliminates the need of time and effort consuming hand digitization of analog records. As the data are formatted as lines separated by a carriage return/line feed, they appear to the data processor as keyboard input and no specialized protocols are required to transfer the data from the cassette recorder to the digital computer.

Figure 5.1 shows a block diagram of the system and describes its various components.

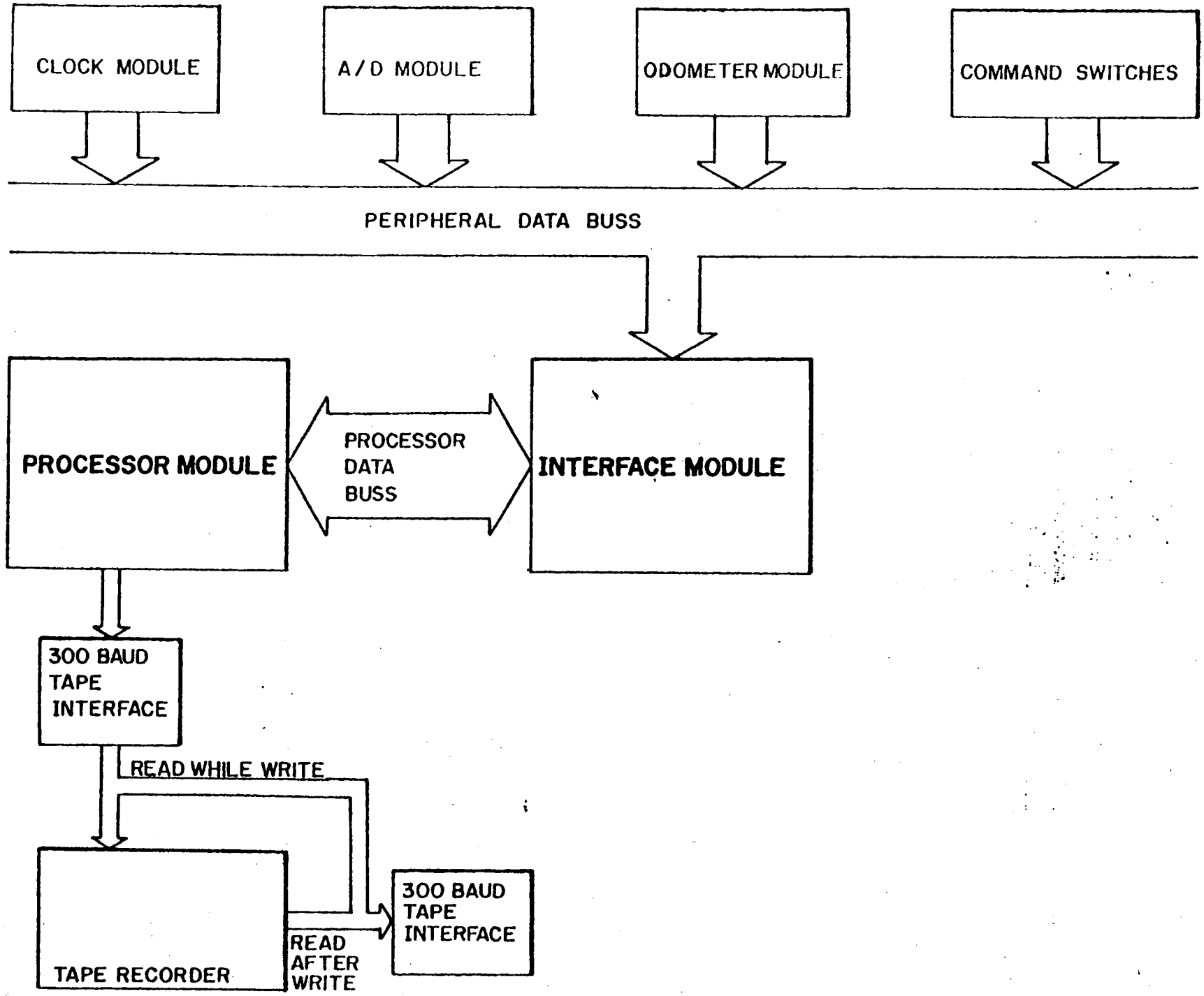

FIGURE 5.1 DATA ACQUISTION SYSTEM BLOCK DIAGRAM

6. DATA COLLECTION

6.1 DATA COLLECTION - METEOROLOGICAL SYSTEMS

6.1.1 Tethersonde

The tethersonde was operated at the approximate height (determined visually) of the plume. It was raised and then simply left until it was time to change the batteries (twice daily). The chart record consists of a plot of various signals vs. time. The data format consists of a sync pulse followed by eight signal pulses, each separated by a zero reference value (Figure 6.1).

The parameters are obtained by measuring the height of the sync pulse which represents a calibrated signal for each sensor. Measuring the signal pulses, determining the ratio and multiplying by the signal range yields the value of the parameter. The pressure is easily converted to height by:

70 cm of Hg = 938.6 mb

Density Hg = 13.6 g/ml

Density Air = .0012 g/ml

$$\frac{\text{Density Hg}}{\text{Density Air}} = \frac{13.6}{.0012} = 11333$$

793333 cm Air = 938.59 mb

100 mb = 84524 cm = 845 m

The full range of pressure (100 mb) represents a height change of 845 m.

The reduced data from the tethersonde was plotted against time to give daily plots of:

1) tethersonde height above ground vs. time
2) tethersonde wind speed vs. time
3) tethersonde wind direction vs. time

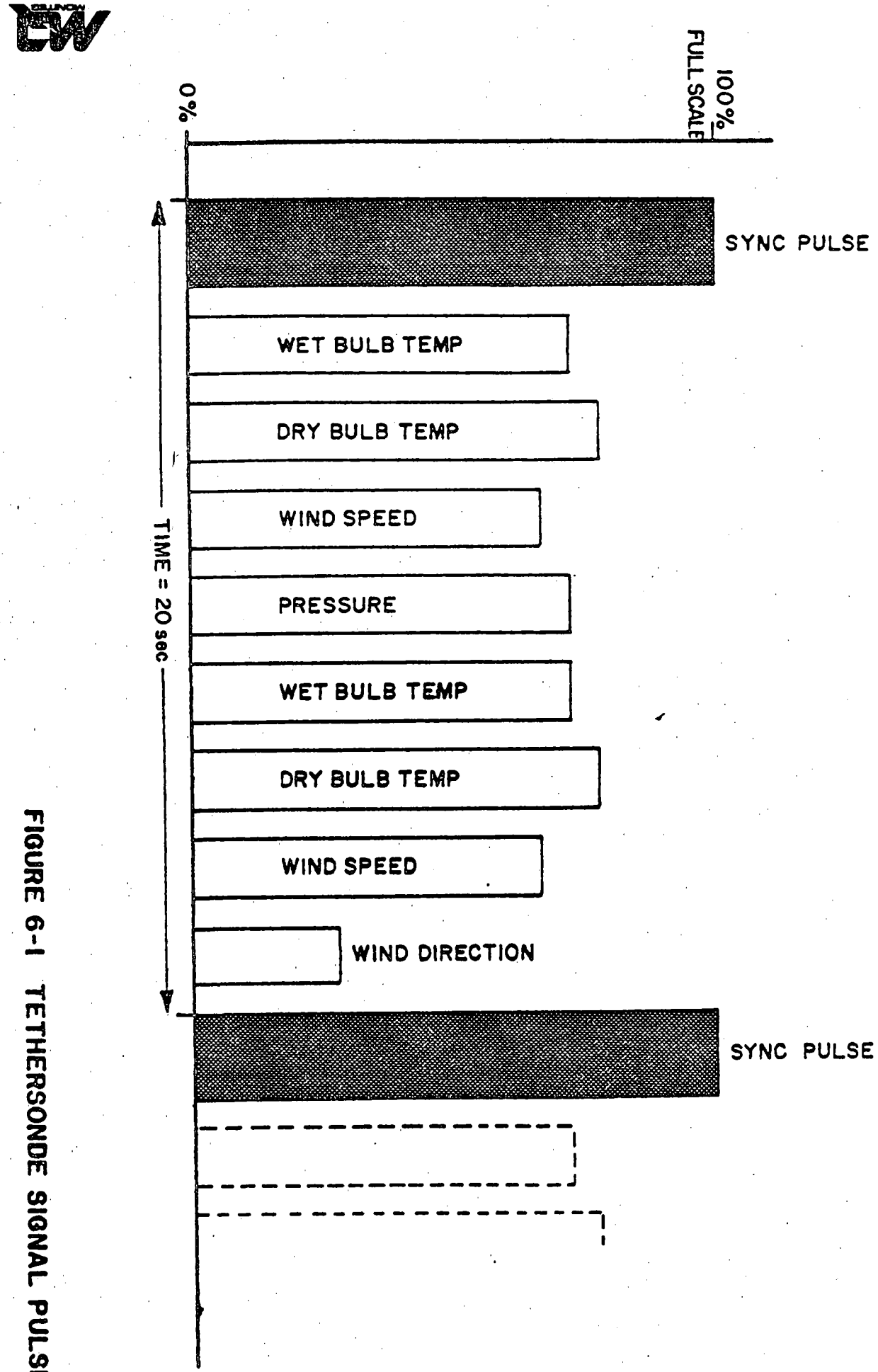

FIGURE 6-1 TETHERSONDE SIGNAL PULSE

6.1.2 The Pilot Balloons

The pilot balloons were released from the base van every 30 minutes. The theodolite readings of azimuth and elevation were dictated by the theodolite operators to portable cassette recorders every 30 seconds and transcribed after the flight. To ensure accurate readings, the theodolites were levelled and aligned in azimuth to each other prior to each flight. The theodolite positions were marked and surveyed to ensure that the exact position could be recovered on geographic maps. These raw data were then inputted to the computer program to yield x, y and z coordinates at 30 second intervals. The height of the balloon and the wind speed and direction during each interval were then determined by comparing consecutive values.

Accurate timing and simultaneous measurements at both theodolite locations were accomplished by communicating with each theodolite operator from the base van on an F.M. two way radio. The operator at the base van communicated the exact 30 second periods by playing into the walkie-talkie communication set a pre-recorded and accurately prepared cassette tape.

The wind speed and direction from the pibal computer output were plotted on the same graph as the tethersonde data to give daily plots of:

4) average pibal wind speed (computed from the vector average over altitude of 100 to 500 m) vs. time
5) pibal wind speed (at height of the tethersonde) vs. time
6) pibal wind direction (computed from the vector average averaged over 100 to 500 m) vs. time
7) pibal wind direction (at the tethersonde height) vs. time

6.1.3 Minisonde System

The minisonde chart record provided a plot of temperature vs. time. From this, the temperature was obtained, and the height vs. time information from the pilot balloon data analysis computer program was used to obtain the plot of temperature changes vs. height. The minisonde was attached to the balloon after initially comparing its ground signal with that of a calibrated thermistor. This ground temperature was added to the temperature difference detected by the minisonde to determine the temperature at a specific time after the launch.

6.2 REMOTE SENSING INSTRUMENTS

Both of the spectrometers were installed in a station wagon and viewed vertically out of the side windows. The power to the equipment including chart recorders, Data Acquisition System, and portable tape recorder was supplied through use of a power inverter connected to the vehicle battery. The chart recorder speed was controlled by the vehicle speed with the use of an intervalometer. The digital data were recorded on tapes in two channels; one containing the odometer reading which is proportional to distance traversed, and the other containing the spectrometer response signal.

Initially, the plume was located by examination of the correlation spectrometer signal on the chart recorder and the horizontal dispersion was estimated. The start and end points of a traverse line were chosen so that they included the whole plume and intersected the plume at as close to 90° as possible.

A sufficient number of passes (10 - 15) were made under the plume within a relatively short time (approximately 30 minutes) to evaluate the data statistically and to remove the effect of large dynamic variations in the concentration profile with height by determination of the mean value. These data were used to determine the average mass flux during that time and to compute a measure of temporal fluctuations during this time interval by determination of the standard deviation. Figure 6.2 shows pictorially the remote sensing method.

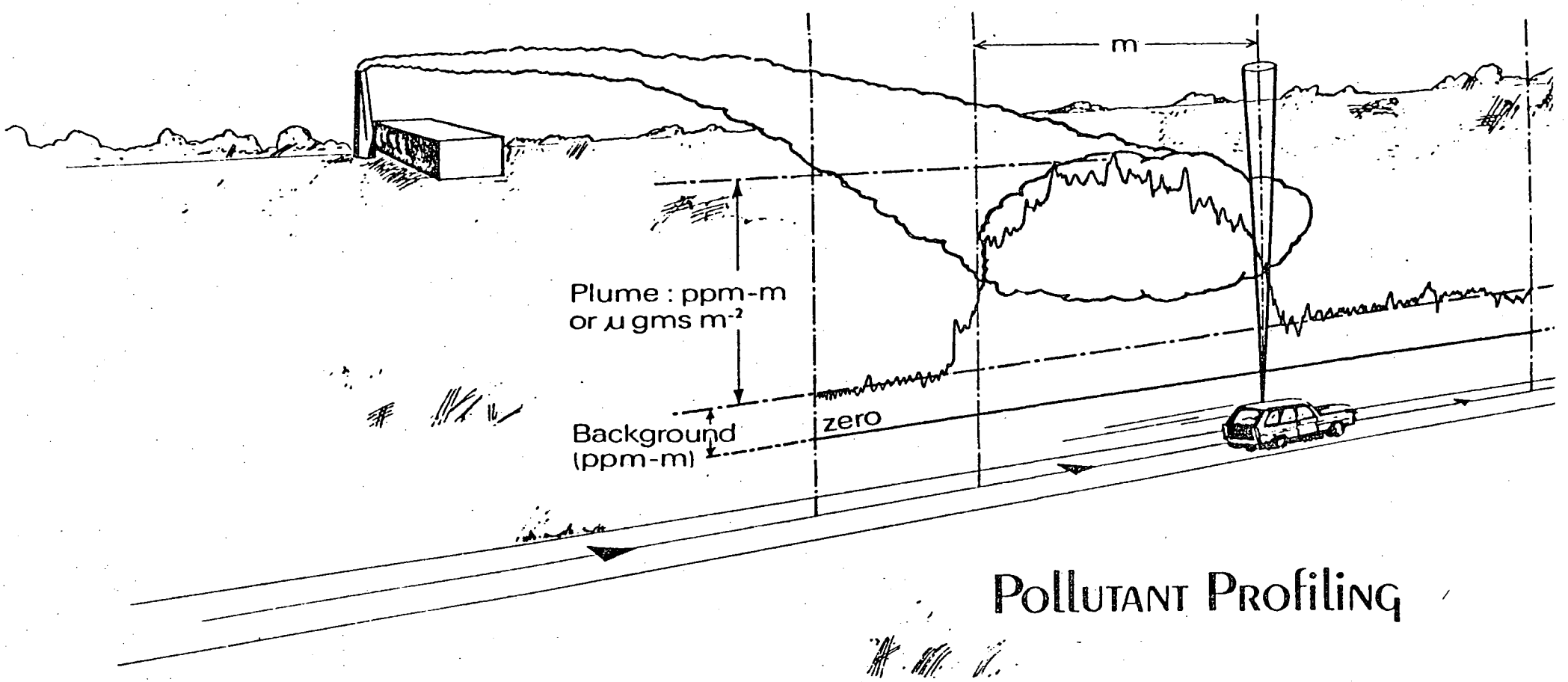

Figure 6.2 THE PLUME PROFILING METHOD

Table 6.1 and Figure 6.3 show a summary of the data collected in the field. The number of traverses made with the remote sensing instruments during various time intervals are shown. The time intervals, when the corresponding meteorological data from the tethersonde and the pilot balloons were available, and when the spectrometer data were recorded on the Data Acquisition System, are also depicted.

6.3 SURVEYING OF THEODOLITE AND VEHICLE TRAVERSE LOCATIONS

The positions of the theodolites were determined by measuring two angles between three known bench marks and comparing these to surveyed maps. Distances were then computed by using geometrical methods. The vehicle traverses were divided into straight line segments on surveyed maps. Traverse segment ends not appearing on the map were determined in the same manner as the theodolite positions. Figure 6.4 and 6.5 show the location of vehicle traverses. The digitized maps were recorded into the computer memory by determining the length and direction of each traverse segment.

6.4 ONTARIO HYDRO METEOROLOGICAL TOWER

Further meteorological data were obtained daily from the Ontario Hydro meteorological station located 12 km NNW of the plant. Measurements of wind speed and wind direction were made. These are also plotted on the daily graphs of wind speed and direction.

SUMMARY OF CORRELATION SPECTROMETER DATA

DATE	LINE	TIME RANGE	LOCATION	NUMBER OF TRAVERSES	DATA ACQUISITION SYSTEM	TETHERSONDE SYSTEM	PILOT BALLOON SYSTEM
Mar. 23	100	953-1008	S. of Stack	6	Off	On	On
	300	1138-1211	S. of Stack	9	Off	On	On
	400	1215-1240	S. of Stack	8	Off	On	Off
Mar. 24	200	1045-1110	S. of Stack	10	Off	On	On
	300	1215-1255	S. of Stack	12	Off	On	Off
	400	1431-1507	S. of Stack	13	Off	Off	Off
	500	1533-1606	S. of Stack	10	Off	On	On
	600	1621-1716	S. of Stack	11	Off	On	Off
Mar. 25	100	813- 842	S. of Stack	10	Off	Off	On
	200	939-1050	Stelco Dock	11	Off	Off	On
	300	1202-1323	Stelco Dock	12	Off	Off	On
Mar. 29	100	933-1036	S. of Stack	11	Off	Off	On
	200	1047-1146	S. of Stack	12	Off	Off	On
	300	1407-1454	S. of Stack	9	Off	On	Off
	400	1533-1629	S. of Stack	12	Off	Off	On
Mar. 31	100	908- 952	1st rd. N. of Hydro	6	Off	On	Off
	200	1000-1029	1st rd. N. of Hydro	8	Off	On	On
	300	1121-1215	1st rd. N. of Hydro	12	On	On	On
	400	1214-1326	1st rd. N. of Hydro	11	On	On	Off
	500	1330-1517	1st rd. N. of Hydro	7	On	On	On
Apr. 1	300	1235	Peacock Pt.	1	On	Off	On
	400	1246-1306	Peacock Pt.	6	On	Off	On
	600	1425-1440	S. of Stack	2	On	Off	On

TABLE 6.1

Summary of the Correlation Spectrometer data collected during the field program.

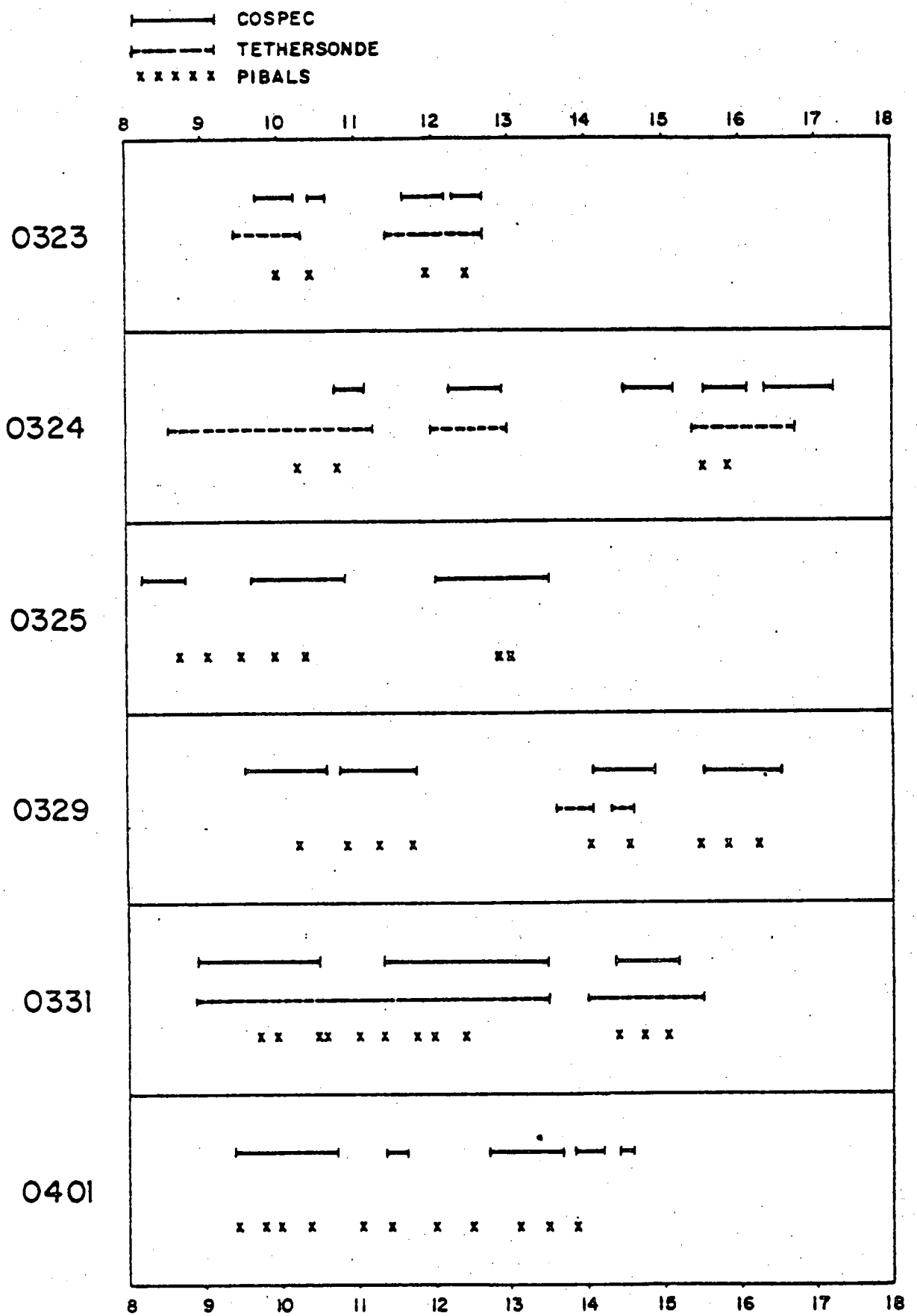

Figure 6.3 SUMMARY OF METEOROLOGICAL AND ENVIRONMENTAL DATA COLLECTED

TRAVERSE LOCATIONS

323 / 101 - 107 (2,3,4,5,6)
108 - 110 (1,2,3,4,5,6)
323 / 201 - 202 (1,2,3,4,5,6)
323 / 301 - 306 (2,3,4,5,6)
323 / 307 - 310 (1,2,3,4,5,6)
323 / 401 - 410 (1,2,3,4,5,6)
324 / 101 - 110
201 - 212
301 - 313
401 - 413
501 - 511
601 - 613
} (6,7,8,9,10)
325 / 101 - 112 (12,8,9,11)
329 / 101 - 112 (1,2,3,4,5,6,7,12)
329 / 201 - 203 (1,2,3,4,5,6,7,12)
329 / 204- (2,3,4,5,6,7,12)
329 / 205 - 213 (1,2,3,4,5,6,7,12)
329 / 301 - 309 (2,3,4,5,6,7,12)
329 / 401 - 402 (2,3,4,5,6,7,12)
329 / 403 - 413 (1,2,3,4,5,6,7,12)

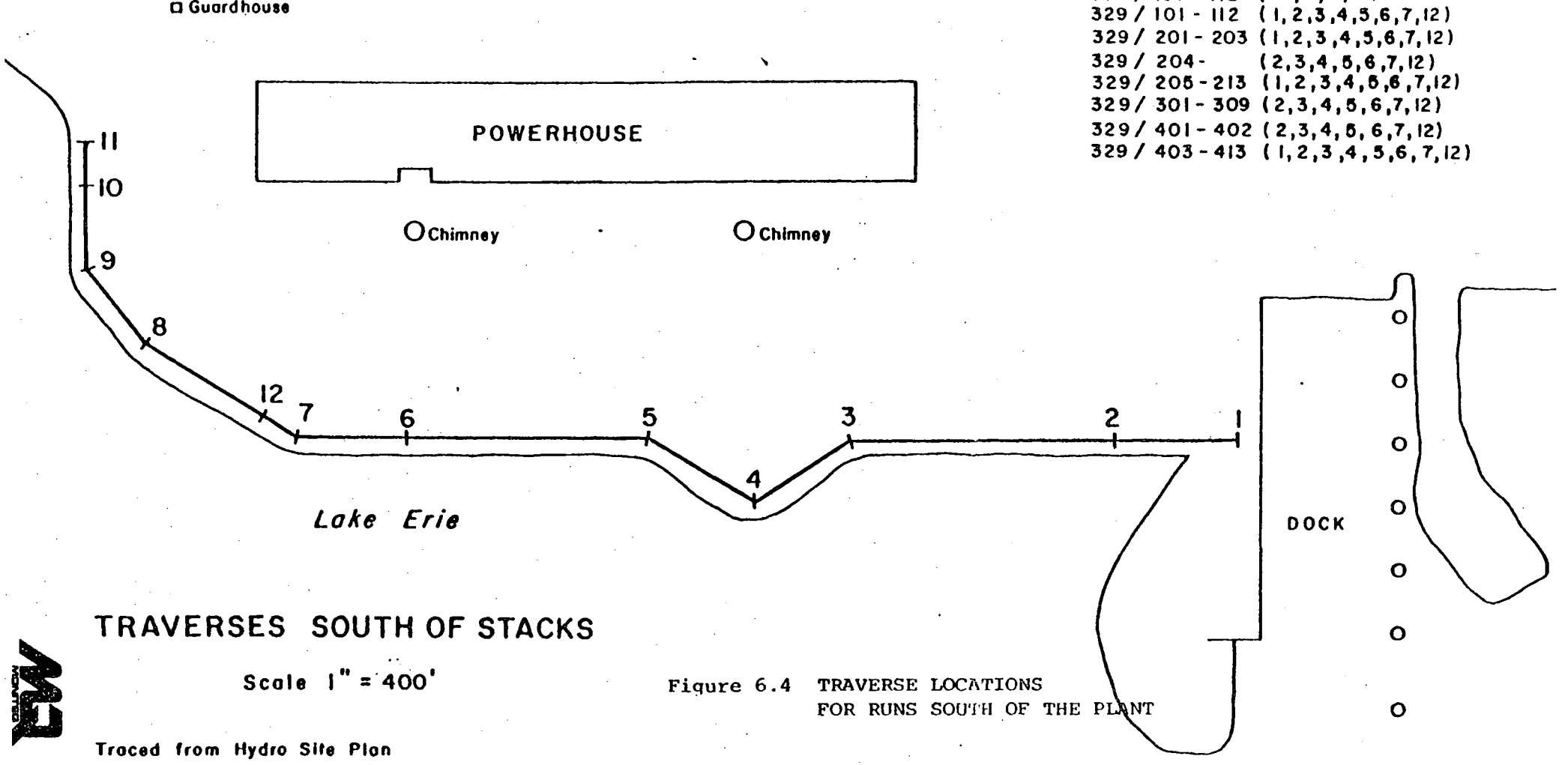

TRAVERSES SOUTH OF STACKS

Scale 1" = 400'

Traced from Hydro Site Plan

Figure 6.4 TRAVERSE LOCATIONS FOR RUNS SOUTH OF THE PLANT

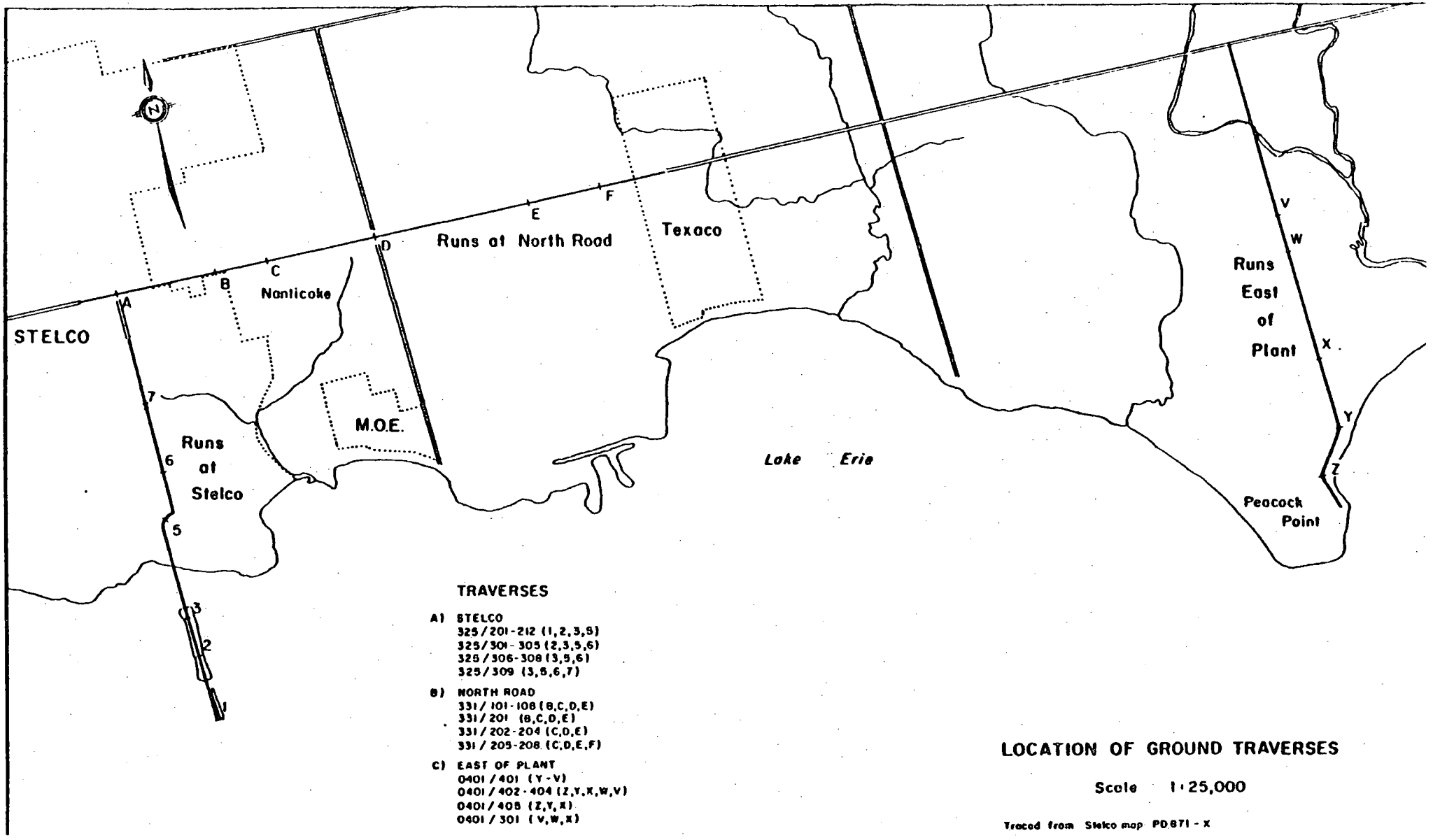

Figure 6.5 LOCATION OF TRAVERSES NORTH, EAST AND WEST OF THE SOURCE

7. DATA ANALYSIS AND INTERPRETATION

7.1 DATA INTERPRETATION METHODOLOGY

The use of a correct methodology is required to interpret the measurement of integrated burdens of sulphur dioxide obtained from a vertical viewing remote sensing instrument. Source emission rates and horizontal dispersion coefficients can be accurately obtained if the data reduction is carefully carried out.

The output from the spectrometer in volts is proportional to the integral along the radiation path of the concentration of SO_2. This output can be expressed in units of concentration times path length, kilograms per square metre ($kg\text{-}m^{-2}$) or parts per million metres (ppm-m).

If the range of vertical plume dispersion is given by the height h_1 to h_2, the correlation spectrometer response will be given by:

$$A = \iint_{v} \int_{h_1}^{h_2} k\,(Z)\,dZ$$

where k(Z) represents the concentration profile with respect to the height above the ground Z.

Under the practical dynamic conditions within the plume, a sufficient number of measurements in time will tend to average out the vertical distribution of the concentration within the range of the plume. For practical application of the instrument, it may therefore be assumed that sufficiently large statistics will yield:

$$A = (h_2 - h_1)k \quad \text{average}$$

The mass flux across any traversed intersection of plume is calculated by computing the area under a profile of spectrometer response ($ppm\text{-}m^2$).

This is done by comparing the measured data to the instrument response for calibration cells containing known burdens of SO_2, and using curve fitting to the calibration curve. The actual traverse is divided into several straight line traverse segments and the distance and direction of each segment is computed. The angle $\emptyset$ between a traverse segment direction and wind direction is computed. Mass flux across a traverse segment is given by:

Mass Flux (kg/sec) = Area under correlation spectrometer response (kg/m) for particular traverse segment
x Wind speed (m/sec)
x Sin $\emptyset$

If N is the number of traverse segments, the total mass flux is given by:

$$\sum_{n=1}^{n=N} \text{Mass Flux (kg/sec)} = \text{Wind Speed} \times \sum_{n=1}^{n=N} (\text{Area})_n \times \text{Sin } (\emptyset)_n$$

The exact mass flux is given by:

$$\text{Mass Flux} = \int_y \int_{h_1}^{h_2} k\ (Z)\ .\ V_{xy}\ (Z)\ .\ dZ$$

which yields

$$\text{Mass Flux} = A\ .\ \frac{1}{h_2 - h_1} \int_{h_1}^{h_2} V_{xy}\ .dZ$$

= Area under the cospec response
x Wind speed vector perpendicular to the traverse direction

Since the vertical dependence of wind speed is also dynamic, it may be possible to use the time average of the wind speed at a specific height within the plume to represent the integrated wind velocity. This is

desirable from a practical viewpoint. In this report, the relative accuracy of using wind velocity measured from a fixed height sensor has been compared with accuracy obtained from a vector average of wind speed over the plume height range. These practical and engineering approximations are necessary to adapt the instrument to operational use and contribute relatively small errors because of the statistical and time-average nature of the analysis.

During this study, it was attempted to obtain a large number of vehicle traverses under the plume within a short period of time. The mass flux was computed for each run, and the average mass flux and its standard deviation were computed. It was also possible to compute the centre of gravity of the plume and the direction of the line connecting the centre of gravity to the stacks was compared with the wind direction.

The meteorological data used to obtain the mass flux were obtained from tethersonde and pilot balloon systems. An average of tethersonde and pilot balloon wind velocity at an approximate plume height was computed and used in the analysis. The analysis was also carried out by using data from the tethersonde alone, and also from a vector average of wind velocity over the altitude range of 100 m to 500 m.

The direction of the line connecting the centre of gravity of the plume to the stacks is another measure of the plume direction. In certain cases, this direction varied by more than 20° when compared to the wind direction used in the analysis. In these cases, the wind direction used in the analysis was altered by a trial-and-error method until the two directions were within 20°. These optimum plume directions, and their difference with the wind direction are presented in Table 8.1.

7.2 METEOROLOGICAL DATA ANALYSIS

The most important objective of this study was the development and evaluation of remote sensing methodology for the determination of mass

emission. From the above discussion, it is apparent that wind speed and wind direction at the plume height should be accurately determined.

7.2.1 Tethersonde Data Analysis

Continuous measurement of wind speed, wind direction, dry and wet bulb temperature and height were made by comparing the signals to the sync. pulse. The sync. pulse magnitude represents a calibrated signal and it was possible during the study to obtain meteorological parameters within the accuracy quoted by the manufacturer. The average value of each parameter for periods of five minutes were computed.

7.2.2 Pibal Data Analysis

The theodolite readings taken at time intervals of 30 seconds were accurately transcribed and coded on computer.

If θ_1, ϕ_1 and θ_2, ϕ_2, are respectively the elevation and azimuth (with respect to the baseline direction), and R_1 and R_2 are respectively the distances of the balloon from two theodolite positions, the following equations hold true:

$$R_1 \cos\theta_1 \cos\phi_1 - R_2 \cos\theta_2 \cos\phi_2 = L$$
$$R_1 \cos\theta_1 \sin\phi_1 = R_2 \cos\theta_2 \sin\phi_2$$
$$R_1 \sin\theta_1 = R_2 \sin\theta_2$$

where L is the distance between the two theodolite positions.

From two of these equations, it is possible to obtain R_1 and R_2 at any moment the theodolite readings are taken. The coordinates of the balloon with respect to either theodolite position can then be found. Comparing the position of the balloon with the position 30 seconds earlier, it is possible to compute the change in the balloon position in the three

orthogonal directions. This change is then used to compute wind speed, wind direction, and average altitude of the balloon. It should be noted that one of the above equations (2nd or 3rd) is redundant and can be used to determine the accuracy and reliability of the data.

In the computation procedure, it is required to know accurately the length and direction of the line connecting the two theodolites. These parameters are computed by surveying the theodolite positions with respect to known bench marks on property maps.

7.2.3 Minisonde Data Analysis

When a minisonde thermistor is attached to the balloon being tracked with two theodolites, it is possible to obtain information regarding altitude of the balloon with respect to time, and signals received by the FM receiver provide temperature profiles with respect to time. From the available data, it was, therefore, possible to obtain altitude-temperature profiles. This information was used to determine if an inversion was present and the altitude of the inversion.

7.3 MASS FLUX CALCULATION BY USING CORRELATION SPECTROMETER DATA

The correlation spectrometer data were recorded initially on chart records, and, later in the field study,with a data acquisition system. Therefore, it was necessary to digitize some chart records prior to processing on a digital computer. Similarly, the map locations were obtained from property maps and from surveyed specific locations.

7.3.1 Acquisition of Geographic Data

From the above discussion, it is apparent that the distance and direction of one pibal theodolite position with respect to the other needs to be

known accurately. Similarly, the start and end points of the vehicle traverses, and the end points of different traverse segments need to be known.

To obtain this information, the property maps, which were made by using previously surveyed data, were used. When the information regarding a specific location which was not on the maps was required, theodolite measurements of three different bench marks were carried out from that location. Use of geometric methods helped graphically plot the specific location. Angles and distances required for analysis were then measured from the maps. It was possible, therefore, to compute magnitude and direction of each traverse segment. The distance and direction of one pibal theodolite position, with respect to the other, were also obtained by using this methodology.

7.3.2 Reduction of Correlation Spectrometer Data

The data recorded on the chart record were obtained by moving the chart paper externally so that the advancement of the chart paper was directly proportional to the distance travelled by the vehicle. The data recorded on tape with the Data Acquisition System were recorded with intervalometer pulse integrator readings on one channel. It was then possible to obtain a profile of the SO_2 burden in ppm-m with respect to the distance on the ground. The SO_2 burden on each traverse segment was computed from the information regarding the magnitude of the traverse segments. The area under the correlation spectrometer response was computed for each traverse segment and the mass flux was obtained by using the meteorological data described in section 7.1.

The correlation spectrometer data recorded on chart paper were digitized by using a commercially available X-Y digitizer and a 9-track computer tape was generated in a card image format. The data files were directly created on the disk space by playing back the data through a cassette interface when they were recorded digitally on cassette tapes.

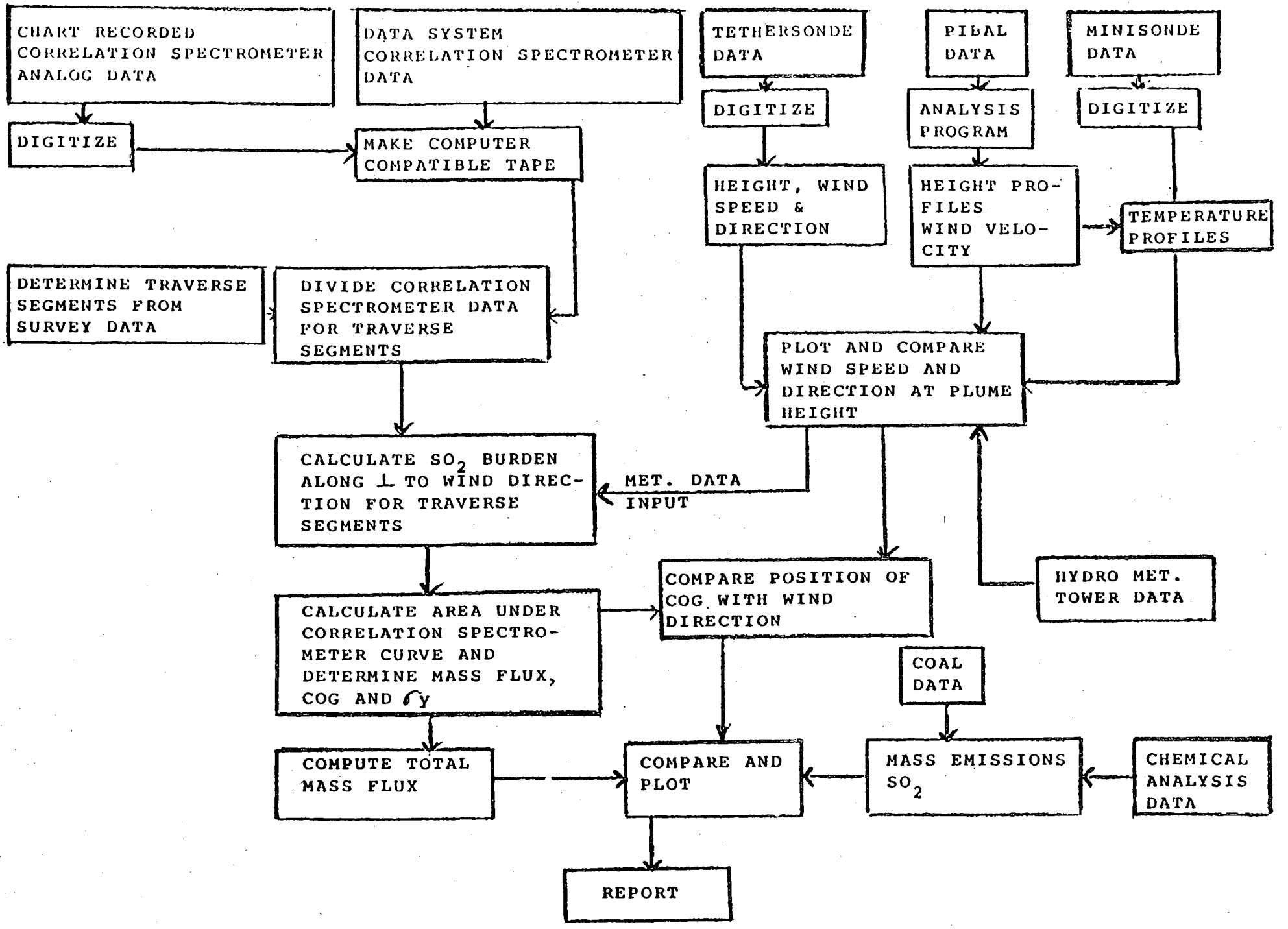

Figure 7.1 A MACROSCOPIC FLOW CHART OF DATA ANALYSIS AND INTERPRETATION

Numerical methods were used to compute the area under the spectrometer response for each traverse segment. Figure 7.1 shows a macroscopic flow chart of the data analysis procedure.

7.4 GAS CELL SPECTROMETER DATA

As previously mentioned (6.2) the gas cell correlation spectrometer, after initial calibration, was operated in a similar configuration to the UV spectrometer. Both instruments were located side by side viewing vertically upwards. The gas cell spectrometer operating at the SO_2 absorption band of 4.0μm in the infrared collected data during 90% of the field program. An evaluation of the instrument's operation was also carried out at night to attempt to define its potential for 24-hour measurement capability. The voltage output from the measurement in emission, is related to the integrated burden of SO_2 in its optical path, in a similar fashion to the correlation spectrometer.

8. RESULTS AND DISCUSSION

8.1 COMPARISON OF DIFFERENT METEOROLOGICAL SENSORS

Figures 8.1, 8.2, 8.3, 8.4, 8.5, 8.6 and 8.7 summarize the meteorological data collected from March 23, 1978 to April 1, 1978. These figures show plots of the tethersonde height, wind speed, and wind direction versus the time of day. The three different sensors (tethersonde, pibals, and instrumented tower at Jarvis) used to measure wind speed and wind direction were then directly compared.

Analysis of the pilot balloon data yielded wind speed and wind direction as a function of its altitude. Since altitude of the balloon with respect to time after launch was also known, it was possible to digitize minisonde data records to yield temperature as a function of altitude. Figures 8.8 to 8.15 show some typical wind speed, wind direction and temperature profiles with altitude.

In figures 8.1 to 8.7, the wind speed and direction from the pibal data were computed by determining the vector average of the wind velocity from an altitude of 100m to 500m. This is considered to be the range of vertical plume dispersion, because the mixing height as determined from the temperature profile data was at approximately 500m. The value of wind speed and direction at the tethersonde height is also plotted.

Whenever possible, it was attempted to fly the tethersonde as close to the plume height as possible. Data from the continuous wind velocity sensor at this height was also plotted and compared to the balloon data. Wind speed and direction measured at the 32m and 85m high sensors located at the meteorological tower situated at about 12 km from the source were also plotted. As the plume was optically visible, its height was easily determined using theodolites.

Figure 8.1 COMPARISON OF METEOROLOGICAL DATA, MARCH 23, 1978

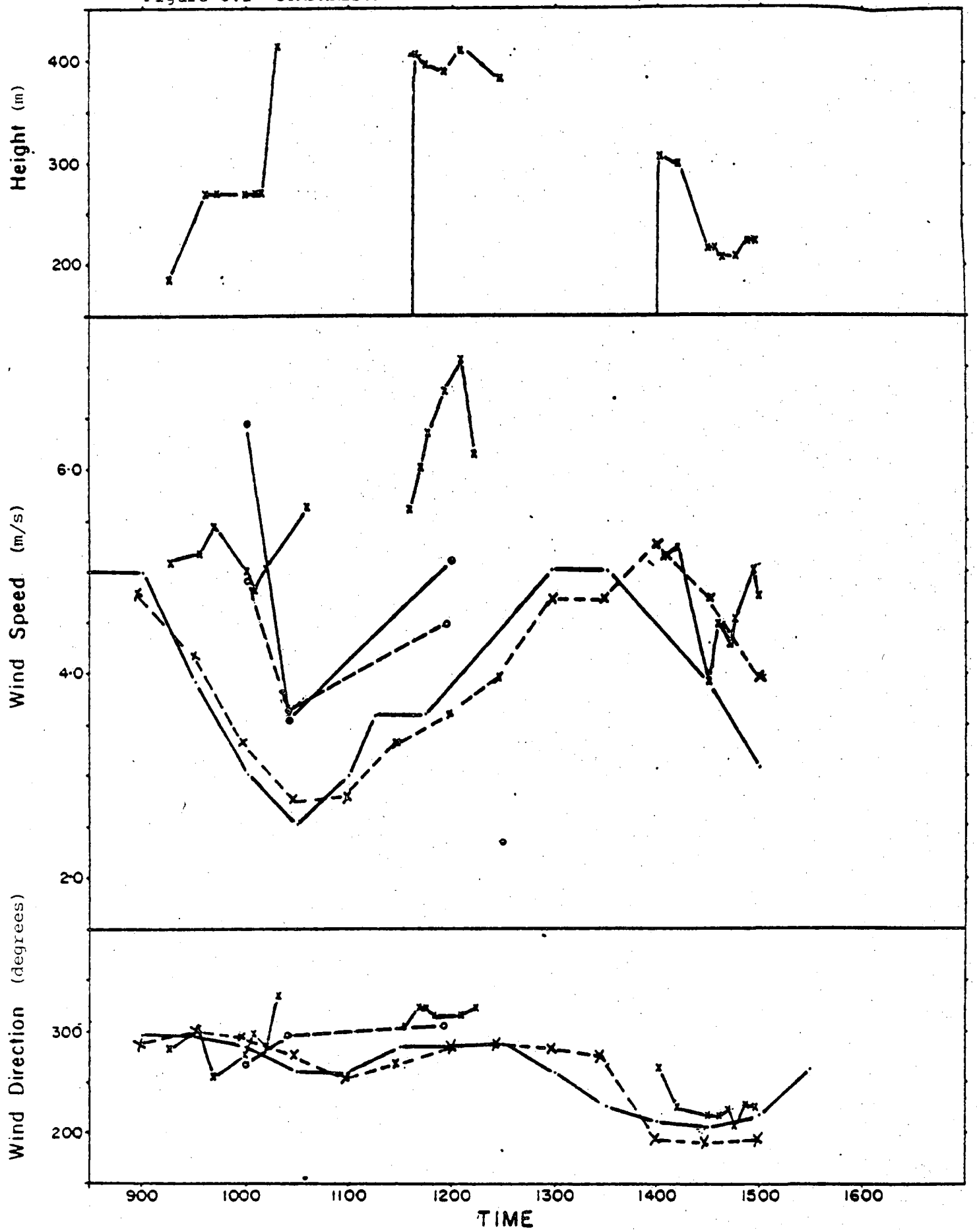

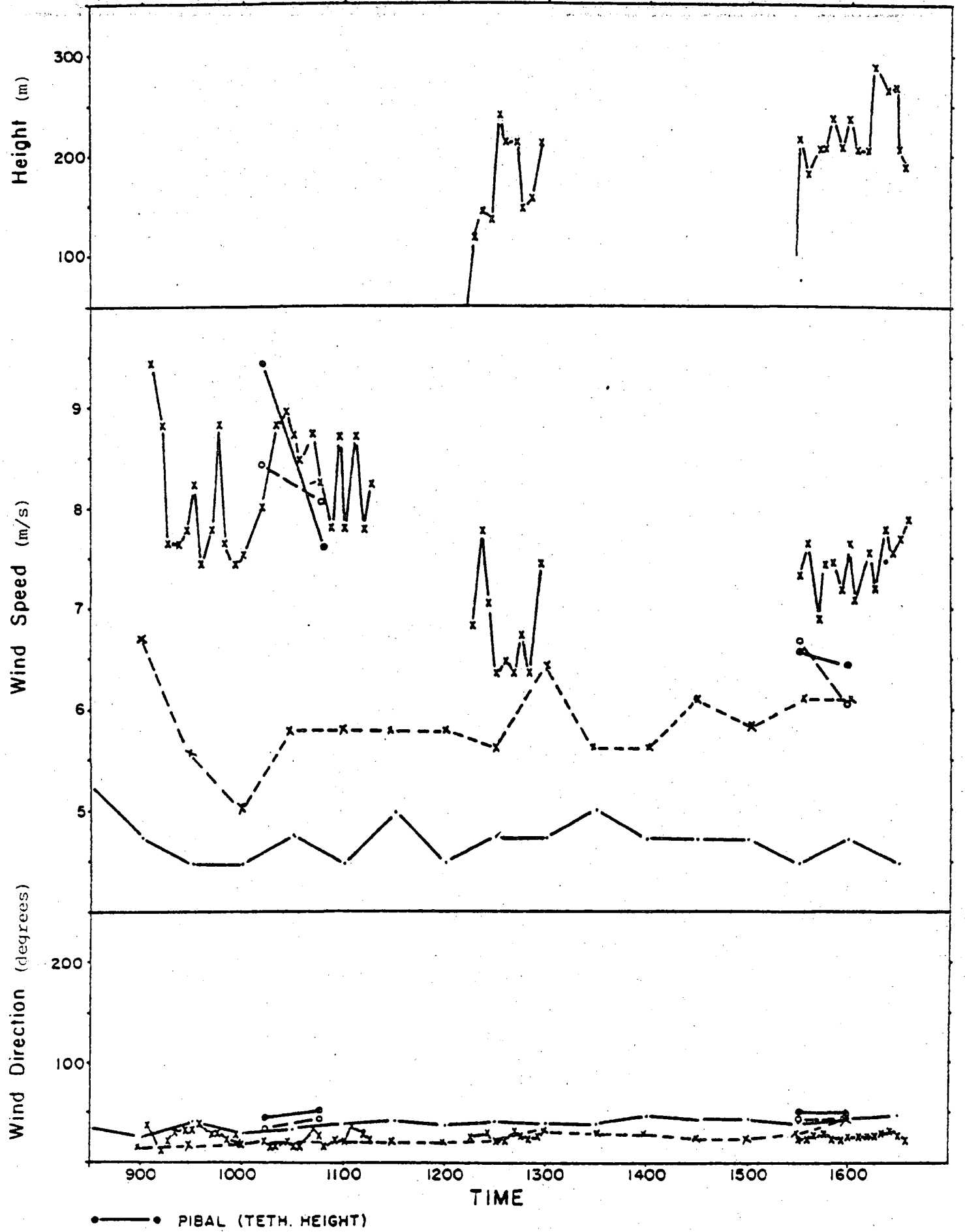
Height (m)
300
200
100
Wind Speed (m/s)
9
8
7
6
5
Wind Direction (degrees)
200
100
900
1000
1100
1200
1300
1400
1500
1600
TIME
PIBAL (TETH. HEIGHT)
PIBAL AVE.
TETHER-SONDE
TOWER (8 Om)
TOWER (32 m)

Figure 8.3 COMPARISON OF METEOROLOGICAL DATA, MARCH 25, 1978

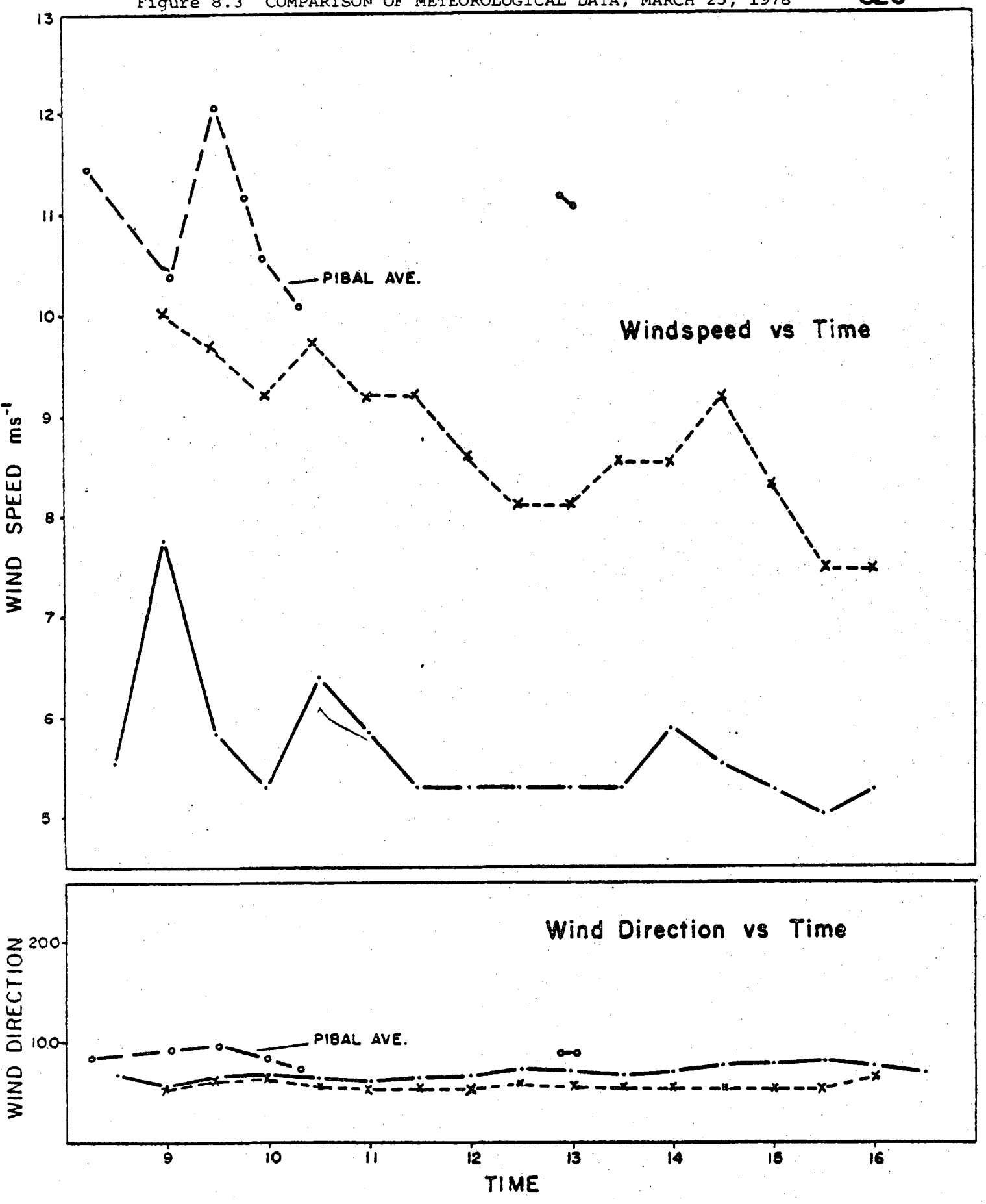

Figure 8.4 COMPARISON OF METEOROLOGICAL DATA, MARCH 29, 1978

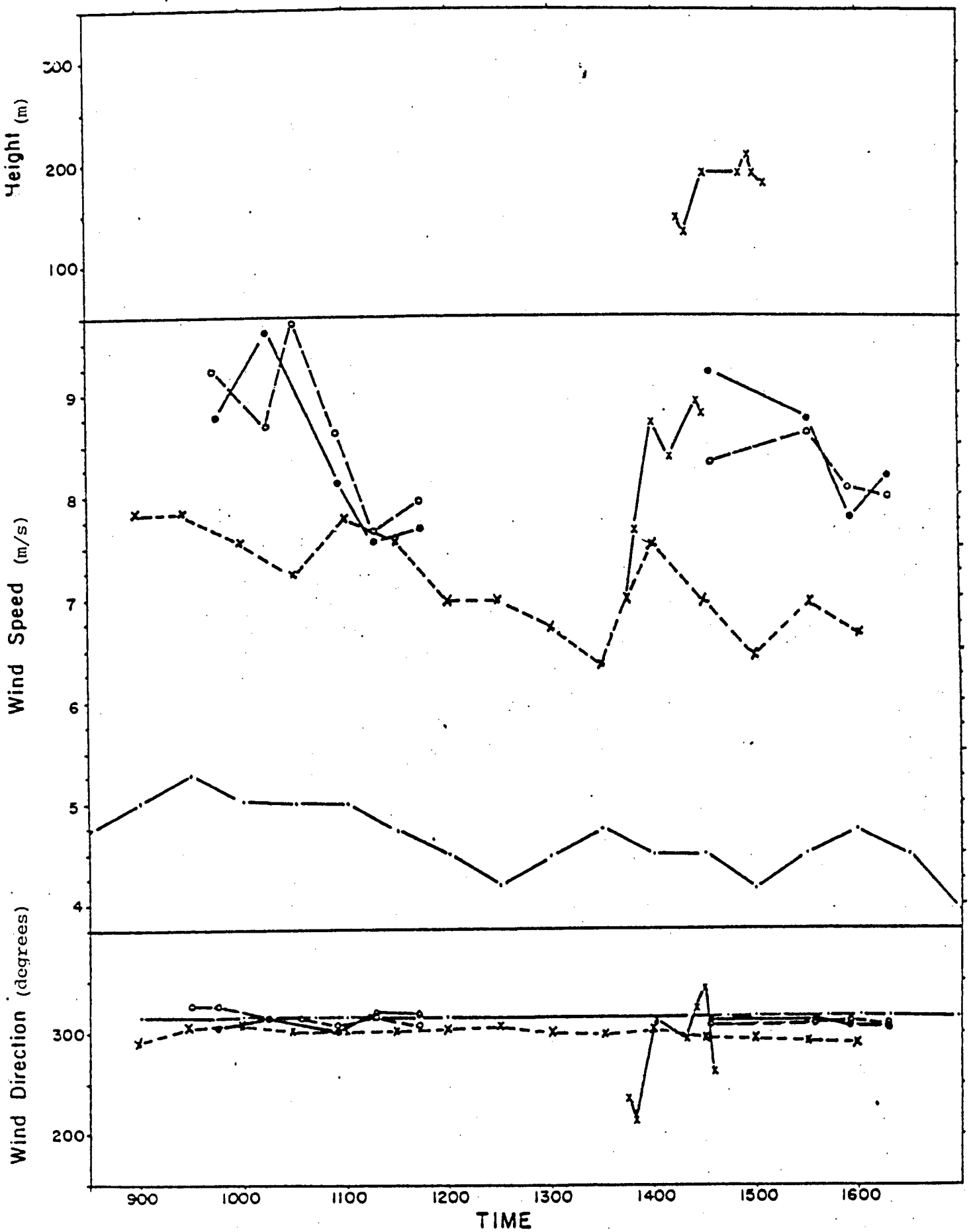

Figure 8.5 COMPARISON OF METEOROLOGICAL DATA, MARCH 30, 1978

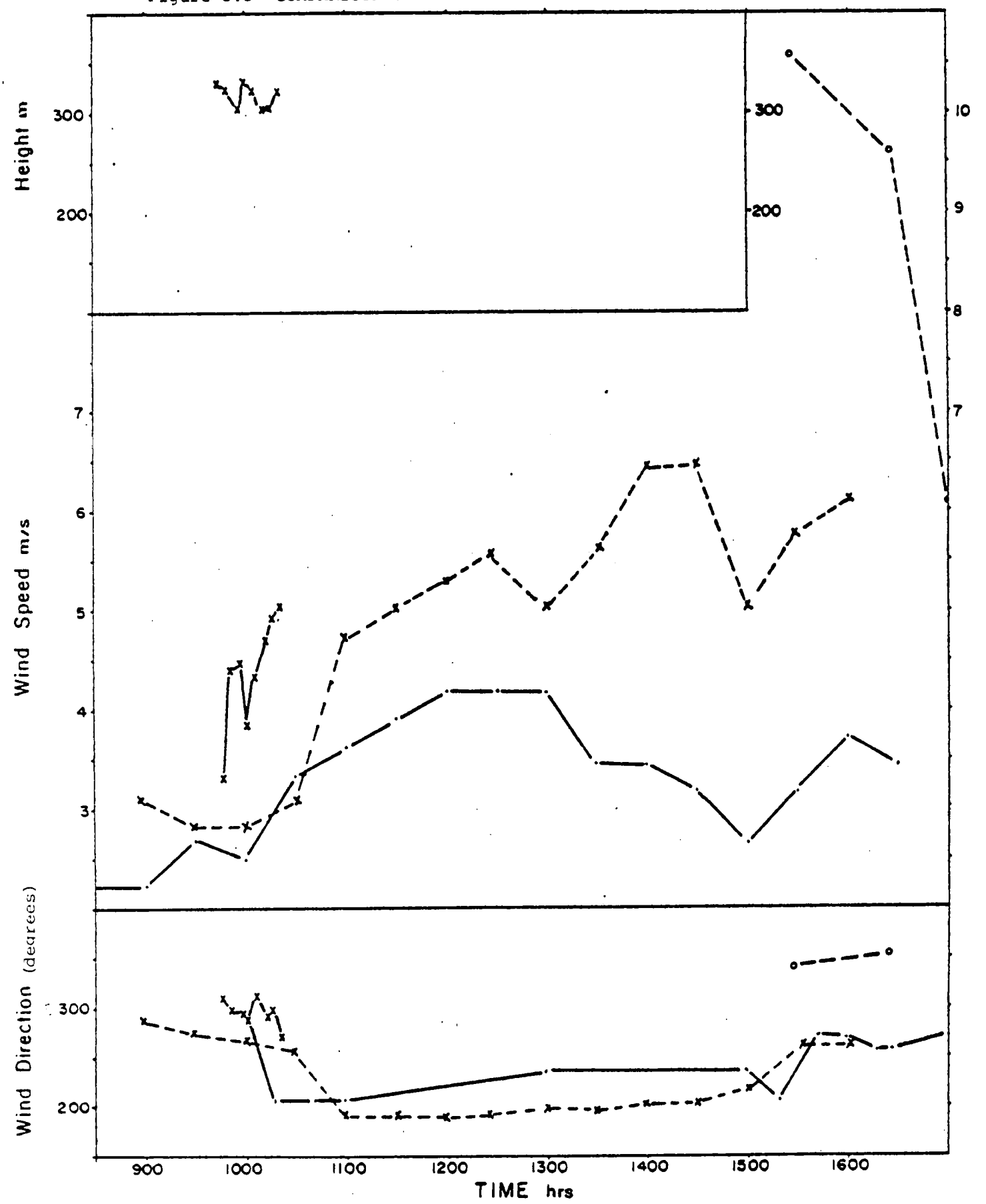

Figure 8.6 COMPARISON OF METFOROLOGICAL DATA, MARCH 31, 1978

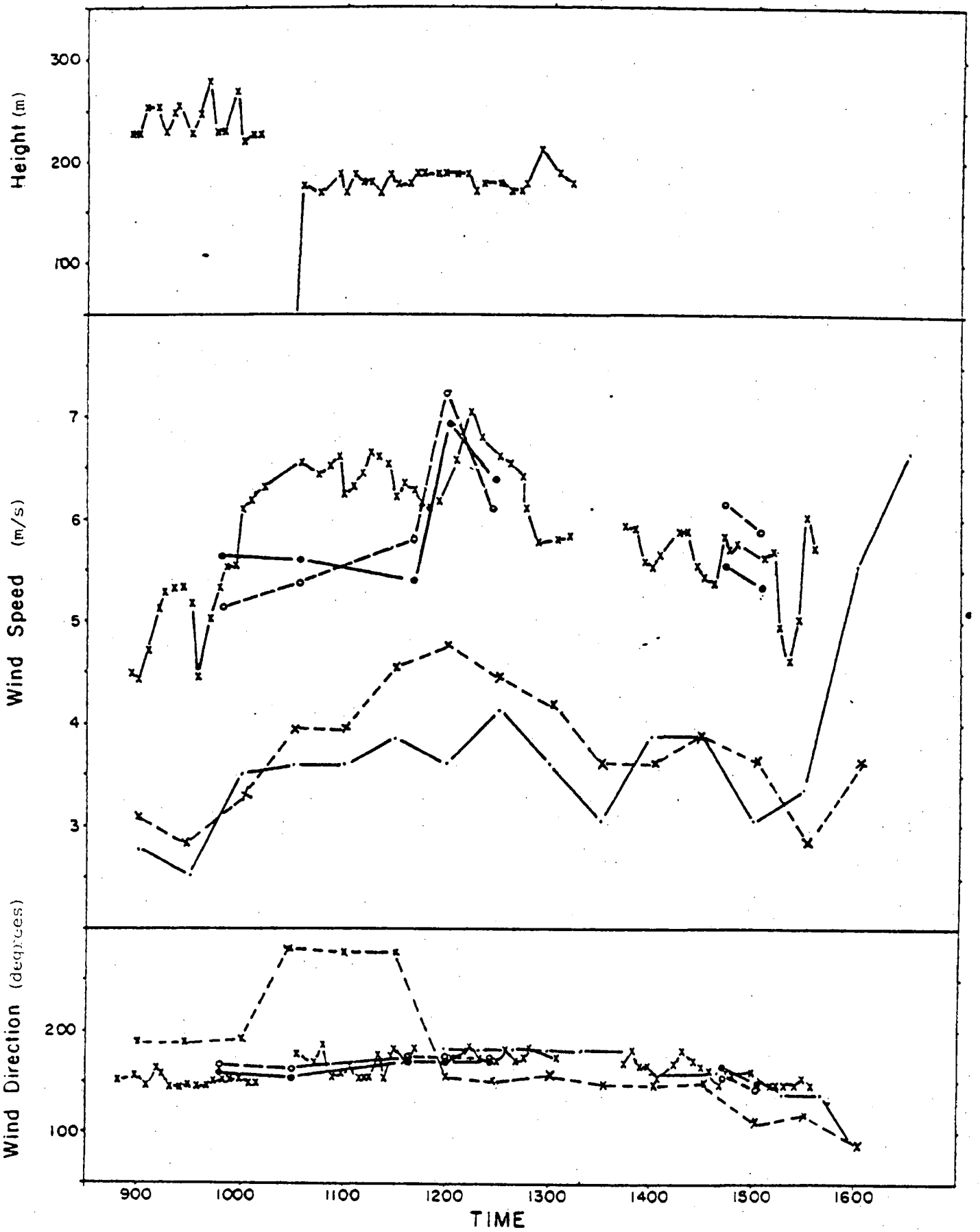

Figure 8.7 PIBAL DATA, APRIL 1, 1978

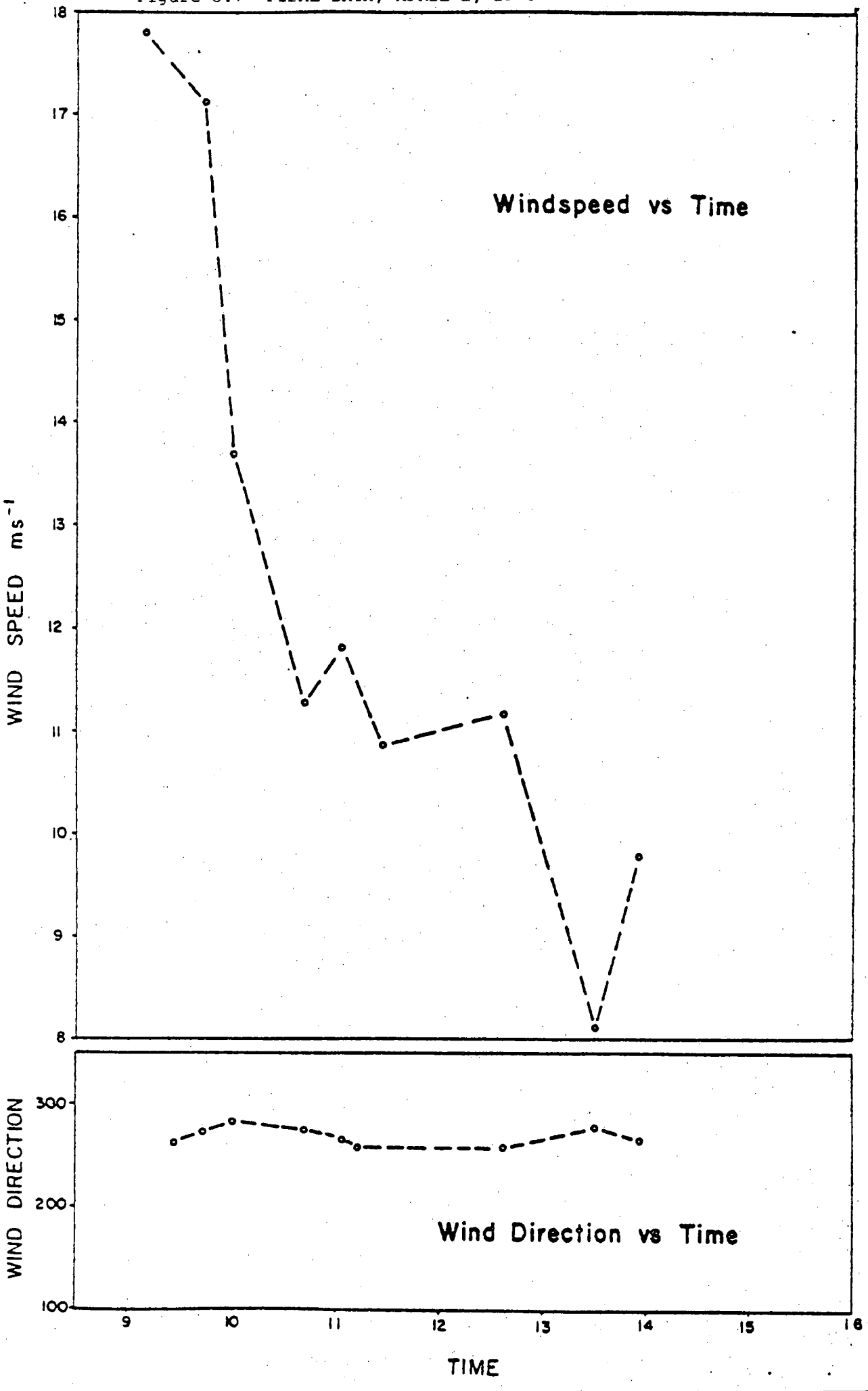

It was found that the wind speed determined from the 85m sensor at the Jarvis tower was consistently lower when compared to pibals or tethersonde measurements (Figure 8.16, Table 8.1). There was no consistent error between the tethersonde and pilot balloon measurements. In most cases, the error in balloon measurements compared to tethersonde data were small.

The wind direction measurements obtained from the Jarvis tower, pilot balloons, and tethersonde compared favourably with each other. However, at selected times, the measurements from different sensors were found to vary by as much as 60°. Further, it was found that the wind direction changed by as much as 90° from 100m altitude to 600m altitude (data from 25th March). Under these wind shear conditions, wind speed and direction measurements from a single fixed height must be carefully evaluated and compared with the plume centre line determined from the remotely measured plume centre of gravity.

The purpose of comparison of different meteorological sensors was to determine the most practical and accurate method to determine wind speed and direction, so that future operational remote sensing missions may be carried out without expending extensive resources to obtain good quality data. It was apparent that the use of an instrumented tower about 12 km from the source did not yield reliable results. The reason for this large disagreement is not yet resolved. The consistency of error in the wind speed measurement at 85m is suspected to be due to instrument calibration errors. Further, the wind speed measured at the 32m level is generally greater than the 85m measurement. This would indicate either a malfunctioning sensor or a calibration error. Until this inconsistency is resolved, the data obtained from the 85m location on the Jarvis tower cannot be used to yield meaningful results. However, it is safe to say that wind direction measured from the tower is within the range of accuracy of other sensors.

In the past, some investigators have utilized one theodolite to track pilot balloons and have assumed the balloon rate of rise to be constant as specified by the manufacturer. Use of a given altitude vs. time relationship and measurements of elevation and azimuth from one theodolite can be used to determine wind velocity. In the absence of atmospheric turbulence and making reasonable assumptions in the equation of vertical motion of the balloon, such a result is valid. For most of our data, the rise rate for a particular balloon was found to be constant within the error of measurement. However, from one balloon to the next, it was found to vary by large amounts. Rise rates of as little as 50m/ min. and as high as 200m/min. were observed by using a balloon with the manufacturer's rate of 180m/min. Since the rise rate depends on the weight of the sonde attached to the balloon and on the amount of helium in the balloon, it is difficult to keep the rise rate the same for each balloon. Therefore, it was considered necessary that the balloon tracking be done with two theodolites to obtain accurate and reliable results.

Flying a tethersonde near the source of pollutant was found to yield continuous, accurate, and reliable results when flown at a constant height in the plume region. Although the measurements of wind velocity and temperature were not known at different altitudes, the simplicity of operation of the equipment and quality of continuous data obtained, outweigh the personnel requirements and complexity of pilot balloon methods. These measurements of wind speed made at a fixed height suggest it will be possible to use tethersonde data alone to provide the complementary input necessary to determine the mass flux. However, it should be noted that it becomes difficult to anchor and to manage tethersondes at wind speeds greater than 12m/sec and during high atmospheric turbulence, especially in restricted or built up areas.

Figures 8.8 to 8.15 also show some selected vertical profiles of temperature determined from the minisondes attached to the pibals. Table 8.1 shows, in tabular form, a summary of the meteorological data.

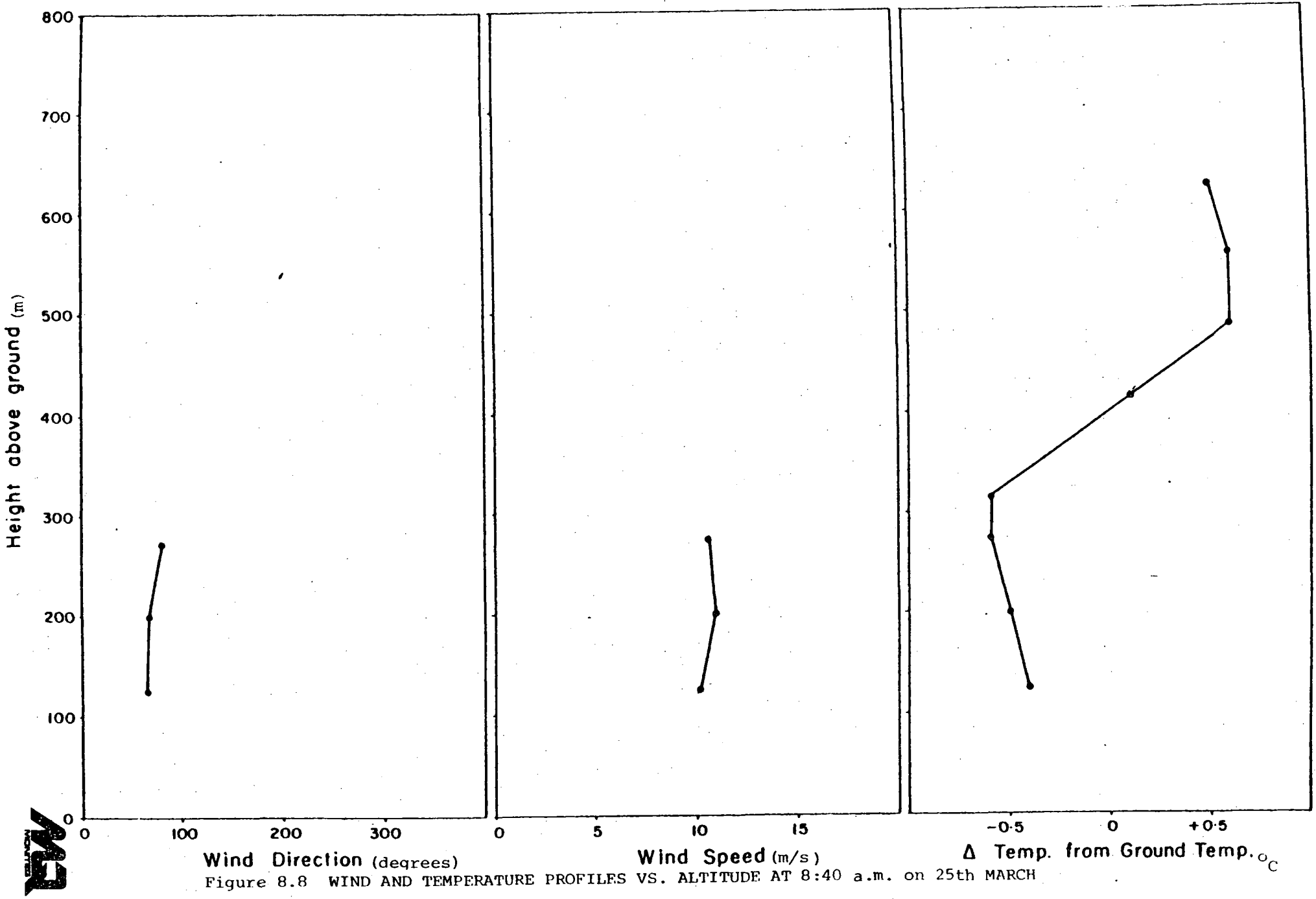

Figure 8.8 WIND AND TEMPERATURE PROFILES VS. ALTITUDE AT 8:40 a.m. on 25th MARCH

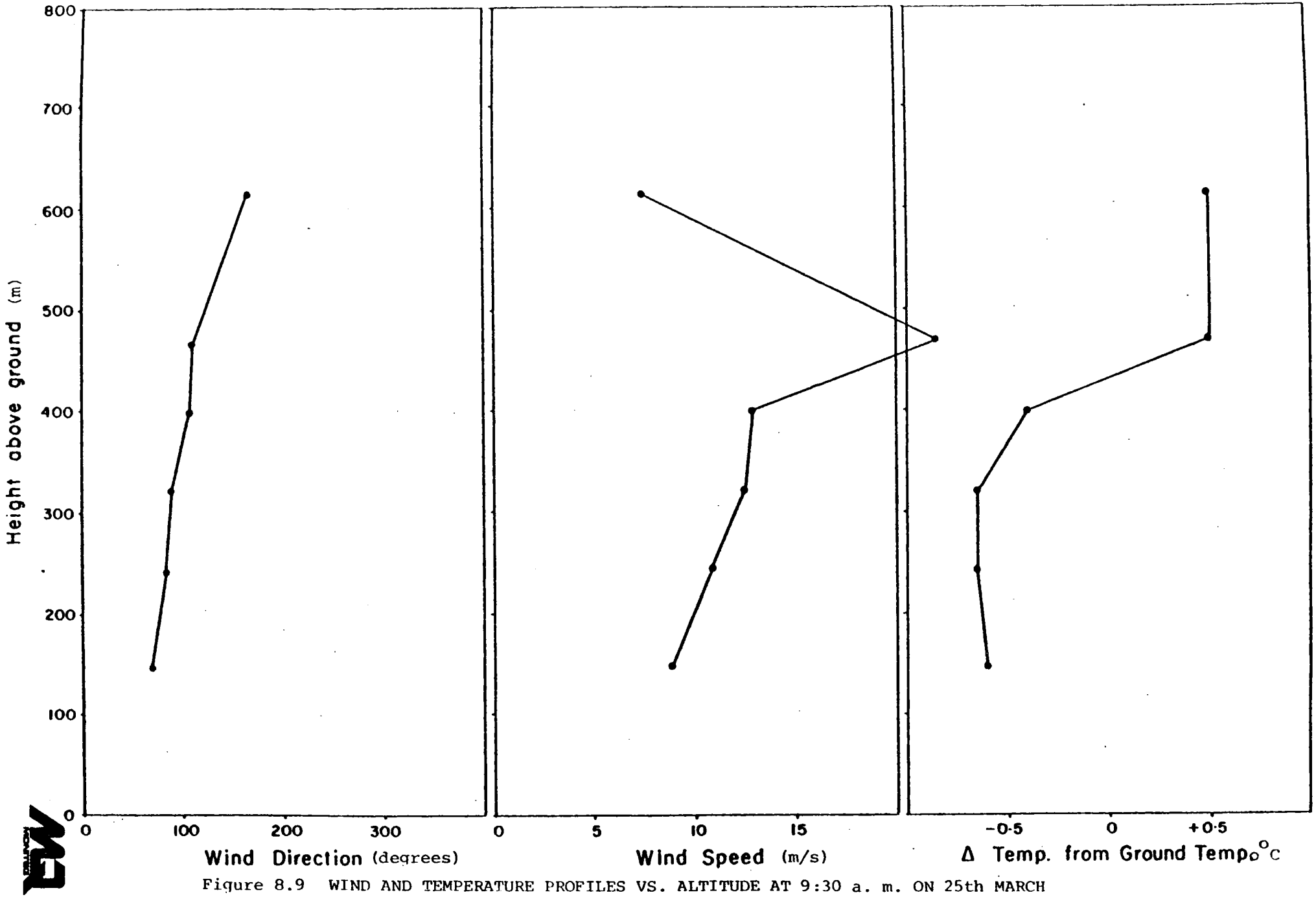

Figure 8.9 WIND AND TEMPERATURE PROFILES VS. ALTITUDE AT 9:30 a. m. ON 25th MARCH

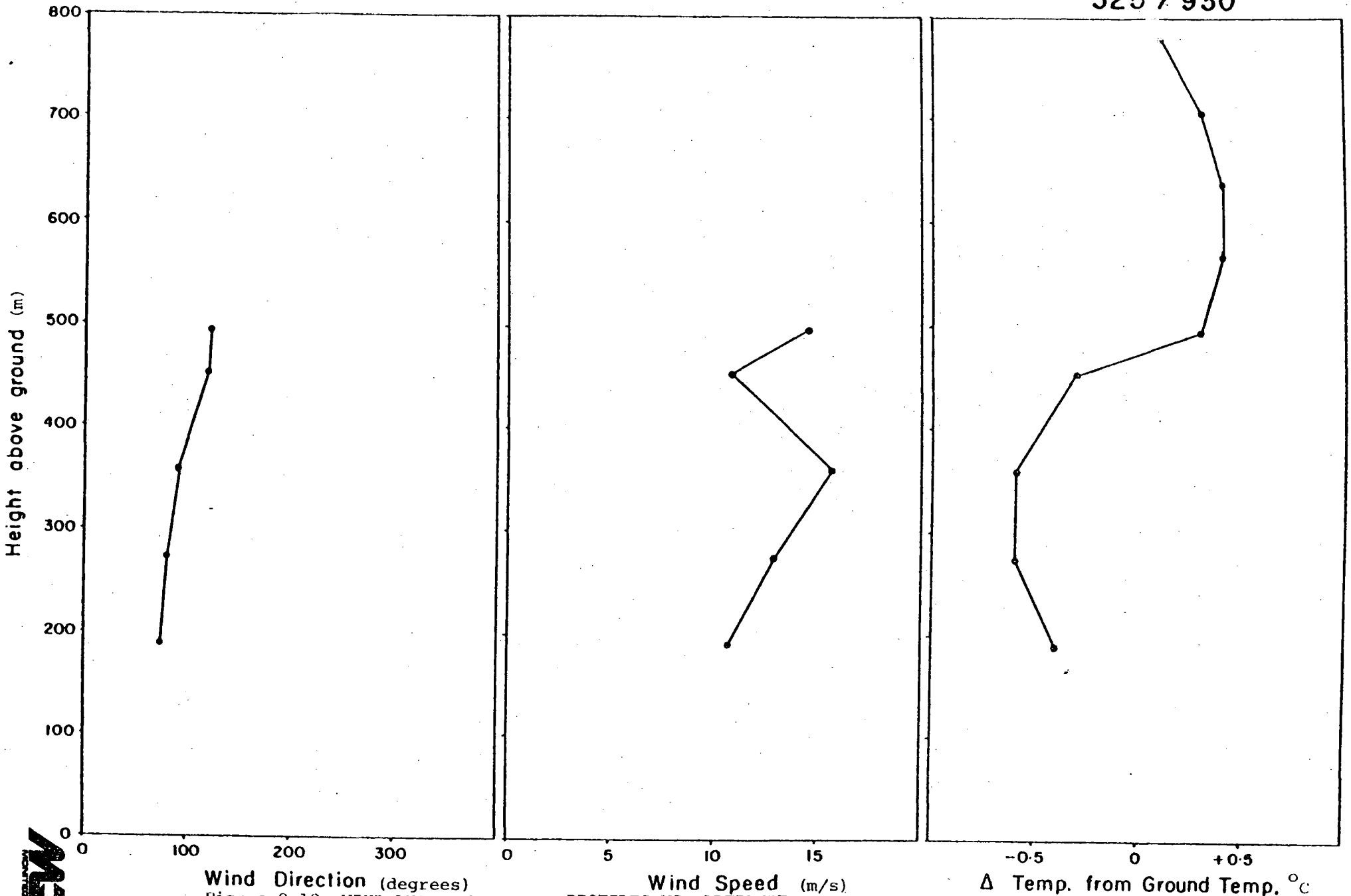

Figure 8.10 WIND AND TEMPERATURE PROFILES VS. ALTITUDE AT 9:30 a. m. ON 25th MARCH

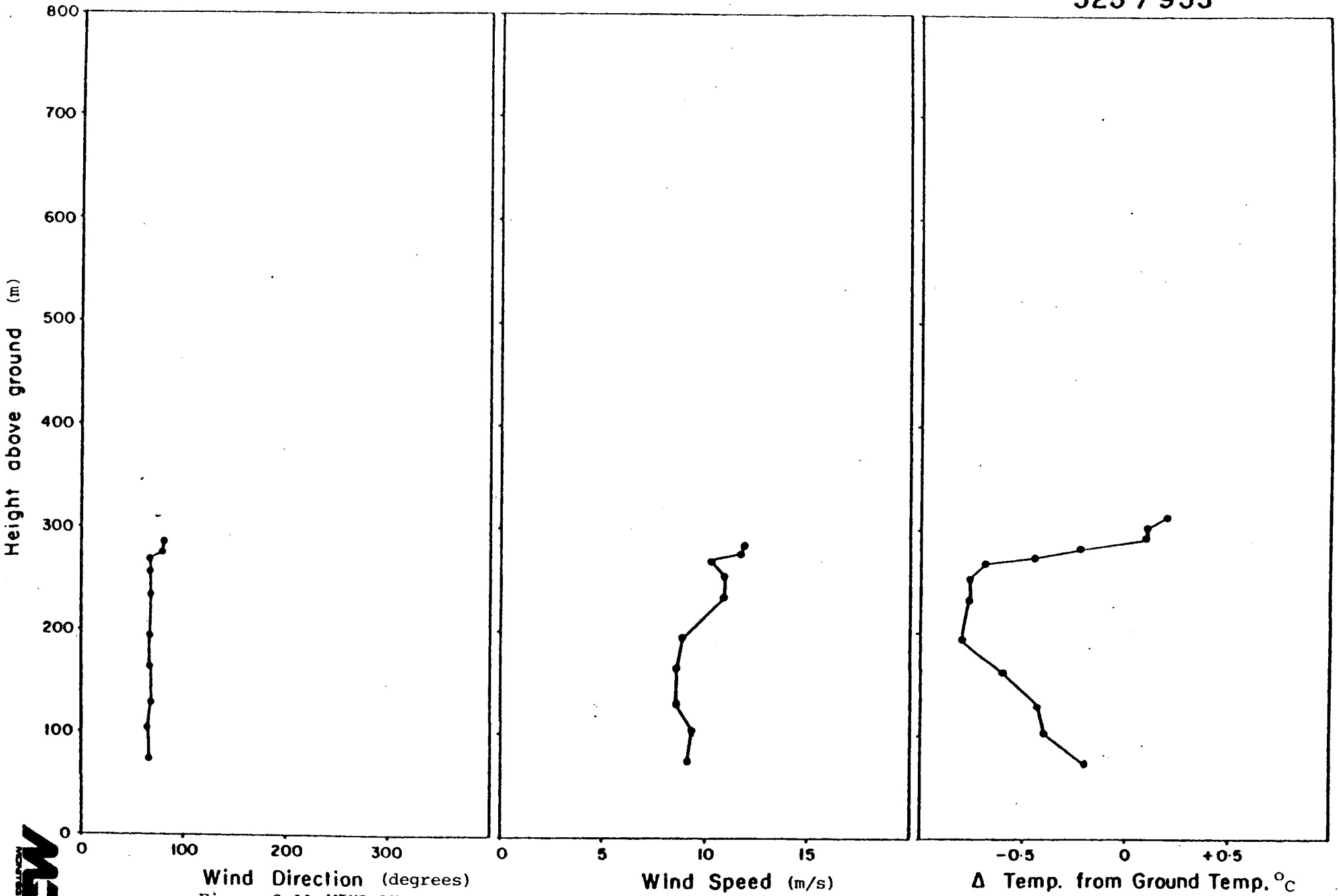

Figure 8.11 WIND AND TEMPERATURE PROFILES VS. ALTITUDE AT 9:55 a. m. ON 25th MARCH

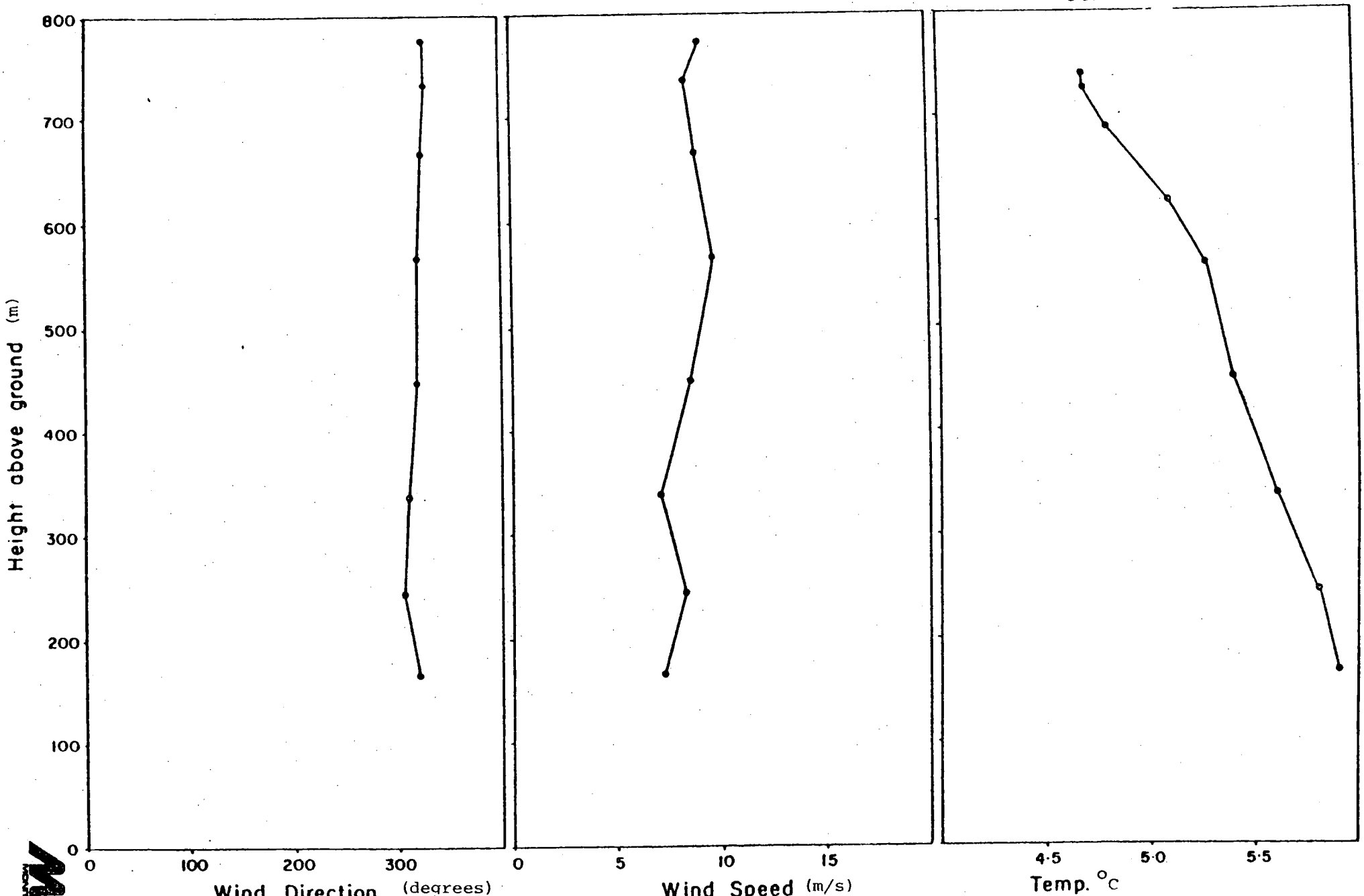

Figure 8.12 WIND AND TEMPERATURE PROFILES VS. ALTITUDE AT 11:16 a. m. ON 29th MARCH

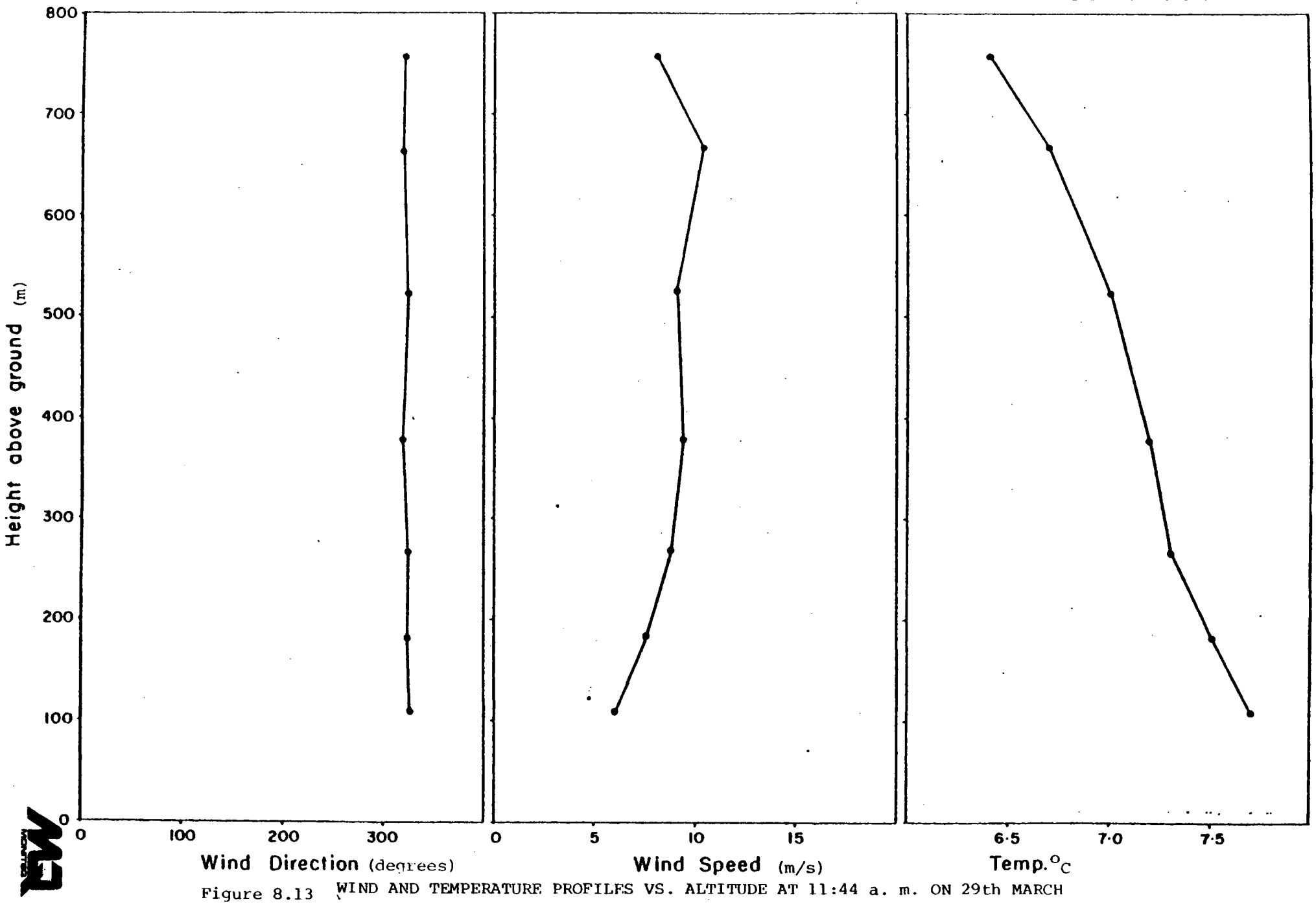

Figure 8.13 WIND AND TEMPERATURE PROFILES VS. ALTITUDE AT 11:44 a. m. ON 29th MARCH

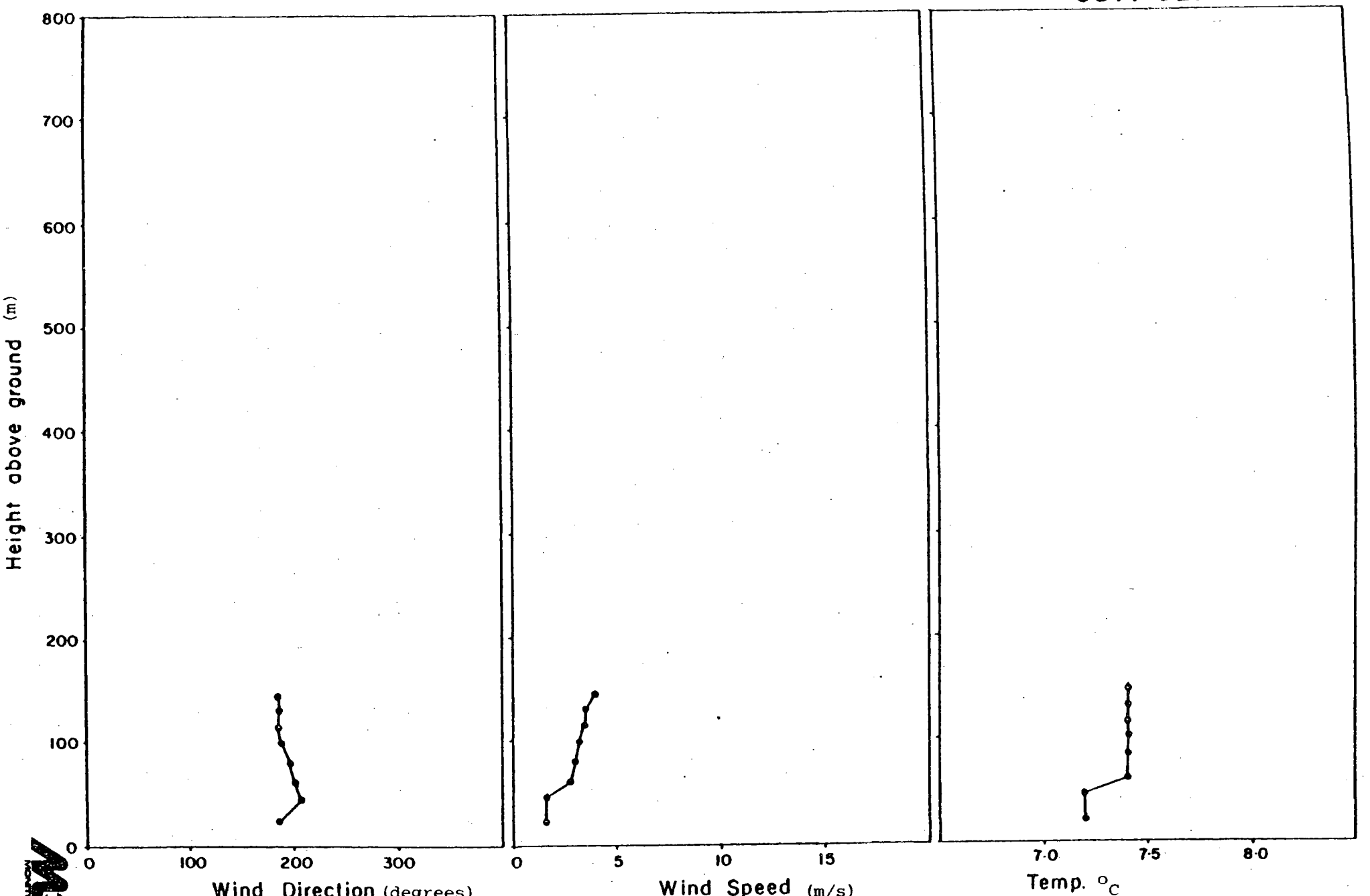

Figure 8.14 WIND AND TEMPERATURE PROFILES VS. ALTITUDE AT 9:22 a. m. ON 31st MARCH

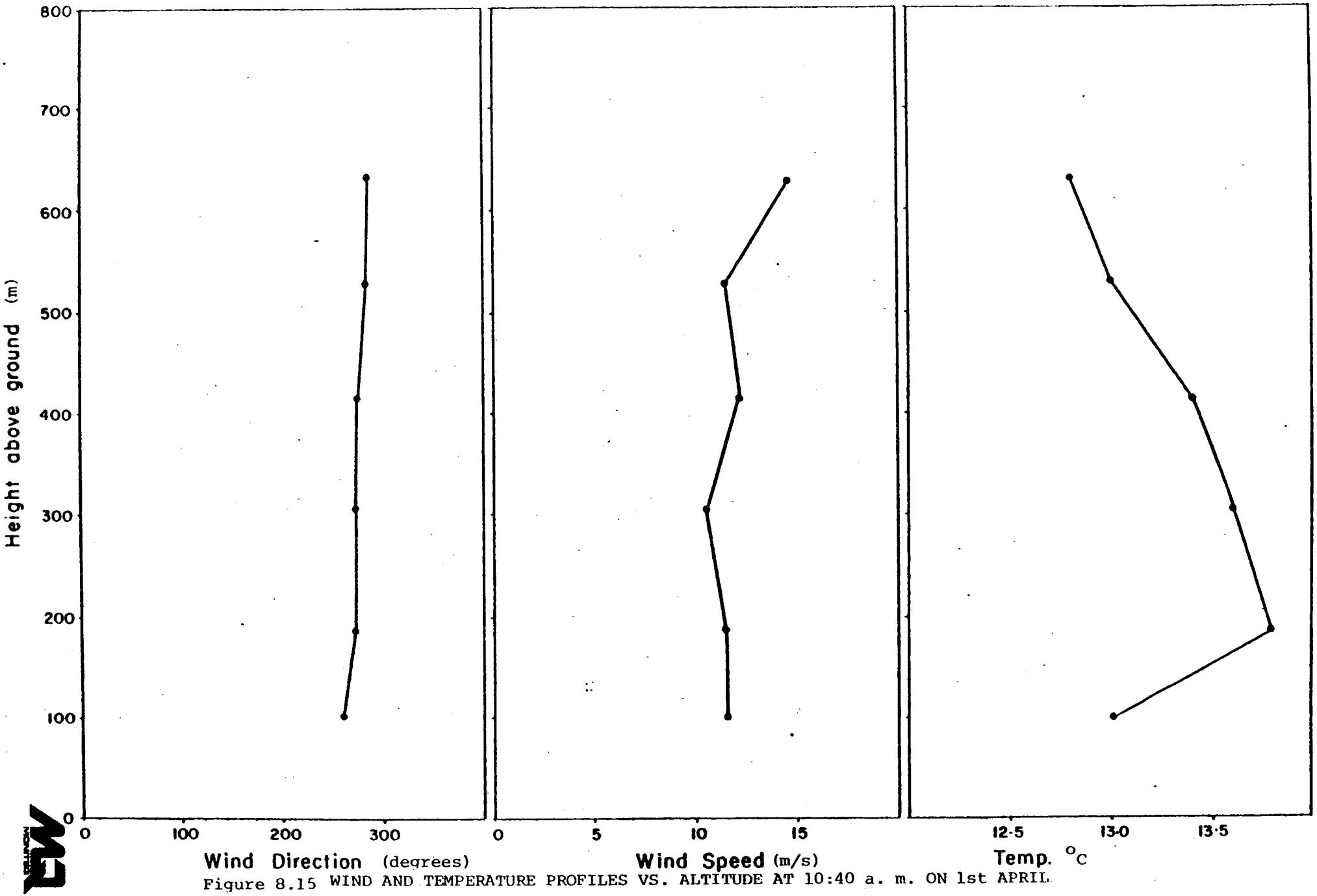

Figure 8.15 WIND AND TEMPERATURE PROFILES VS. ALTITUDE AT 10:40 a. m. ON 1st APRIL

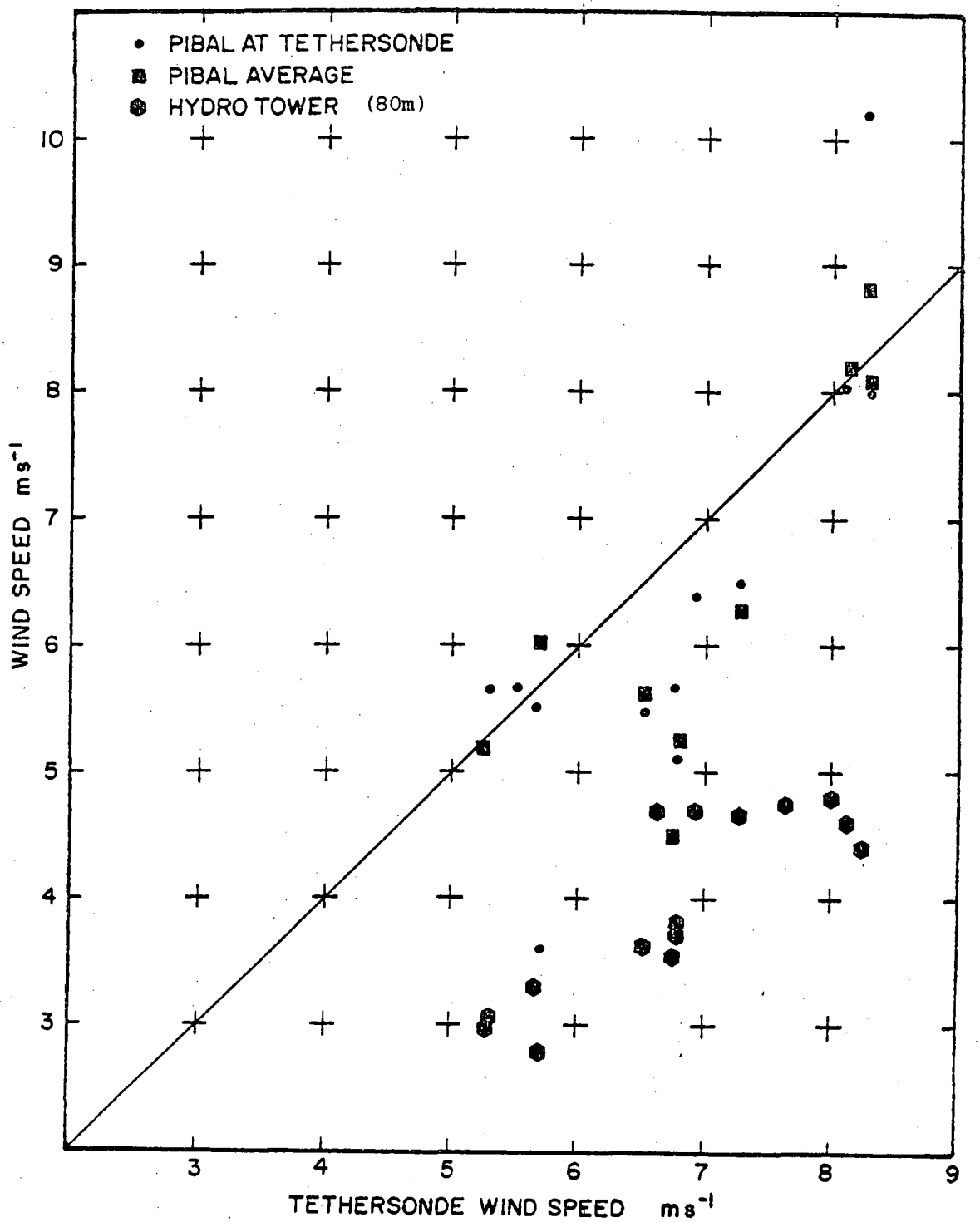

Figure 8.16 COMPARISON OF WIND MEASUREMENTS (WINDSPEED VS TETHERSONDE WINDSPEED)

DAY/LINE CODE	TIME	T'SONDE AT PLUME HT m/s	deg^{o}	MET TOWER m/s	deg^{o}	PIBAL VECTOR AVERAGE 100 - 500 m m/s	deg^{o}	PIBAL AT PLUME HT m/s	deg^{o}	TIME INTERPOLATED WIND SPEED AVERAGE OF PIBAL AT T'SONDE HT.	OPTIMUM PLUME DIRECTION	Δ ANGLE^{o} PLUME DIRECTION & COG
323/100	941-1008	5.2	285	3.0	275	4.9	270	6.4	270	5.6	300	- 10.5
323/300	1138-1211	6.75	315	3.75	285	4.5	305	5.1	300	6.0	300	- 7.5
323/400	1215-1240	-		4.7	280	4.6	310	-		5.9	310	+ 10
324/200	1045-1110	8.25	20	4.8	30	8.1	40	8.0	40	8.15	40	- 18
324/300	1215-1255	6.6	25	4.7	40	-		-		6.6	40	- 18
324/400	1431-1501	6.9	25	4.7	45	-		-		6.9	45	- 10
324/500	1533-1606	7.25	25	4.65	45	6.25	45	6.5	50	6.75	50	- 7.5
324/600	1621-1716	7.6	30	4.7	45	-		-		7.2	50	- 9
325/100	813- 842	-		6.39	65	11.1	85	10.2	80	10.2	70	- 1.5
325/200	939-1050	-		5.3	85	11.1	75	9.6	65	9.6	70	- 9
325/300	1202-1323	-		5.3	80	11.1	80	9.5	70	9.5	70	+ 11
329/100	933-1036	-		5.05	315	8.9	315	-		8.9	315	+ 7
329/200	1047-1146	-		4.75	315	7.9	310	-		7.9	315	+ 5
329/300	1407-1454	8.25	290	4.4	315	8.3	310	10.2	315	8.8	290	- 4
329/400	1533-1629	-		4.6	315	8.2	310	-		8.2	315	+ 7
331/100	908- 952	5.5	150	3.0	170	5.2	160	5.65	170	5.5	160	+ 2
331/200	1000-1029	6.75	150	3.55	170	5.25	160	5.65	160	6.1	160	+ 10
331/300	1121-1215	6.6	175	3.65	180	7.0	160	6.7	160	6.75	175	- 5
331/400	1215-1324	6.75	175	3.75	180	-		-		6.75	175	+ 18.5
331/500	1330-1509	5.65	160	3.3	160	6.0	145	5.5	150	5.6	160	+ 15
401/300 +400	1246-1306	-		6.67	270	9.0-11.1,260		9.0-11.1,260		9.0-11.1	260	+ 9.5
401/600	1425-1440	-		9.45	285	-		-		10.2	290	- 4

TABLE 8.1

Comparison of meteorological data obtained from different sensors employed in this project.

8.2 COMPUTATION OF THE TOTAL MASS FLUX FROM THE HYDRO PLANT

The methodology discussed in chapter 7 was used to determine the total mass flux of sulphur dioxide through a vehicle traverse cross-section. At the locations where the ground traverses were carried out <10 km from the source and under the local meteorological conditions (no measurable plume impingement taking place) removal of SO_2 from the plume due to deposition and/or chemical transformation may be neglected. The computed mass flux should then equal the rate of mass emission.

Mass emission was computed using remote sensing for each traverse under the plume and Appendix 1 lists the data obtained. A number of traverses taken during a short time interval ($\sim$30 minutes) at the same location were averaged and the standard deviation of the mass flux was computed. These data were then compared with hourly averages of sulphur dioxide mass emission determined by computing the mass balance of the sulphur content in the coal burned.

Tables 8.2, 8.3 show a summary of data obtained during the 6 days when it was possible to make measurements. Figures 8.17, 8.18 and 8.19 show the same data in graphical form. For figure 8.17 and Table 8.2, the wind speed and direction were computed from time interpolated average of tethersonde wind velocity and pibal wind velocity at tethersonde height. For figure 8.18, the wind velocity was taken from the tethersonde, while for figure 8.19, a vector average of the value of wind velocity from 100 m to 500 m was used. The continuous line data plotted was obtained from the Ontario Hydro calculation of mass emission based on the total power generated, fuel consumption at that load, and sulphur content of coal determined from chemical analysis once per week. The bars shown on remote sensing data are extended by one standard deviation on each side of the mean in y axis and by the time interval of measurements in x axis.

DAY/LINE CODE	TIME	NUMBER OF TRAVERSES	DISTANCE TO TRAVERSE	WIND SPEED MASS FLUX CALCULATION AVERAGE OF T'SONDE & PIBAL DATA AT PLUME HT.	HYDRO MASS EMISSIONS	MASS FLUX CALCULATED USING WINDSPEED FROM AVERAGE OF T'SONDE & PIBAL DATA AT PLUME HT.	MEASURED-HYDRO / HYDRO % ERROR
			M	M/S	kg/sec	kg/sec	
323/100	941-1008	6	300	5.6	9.15	9.90 ± 1.17	+ 8.2
323/300	1138-1211	9	300	6.0	9.30	9.75 ± 1.41	+ 4.84
323/400	1215-1240	8	300	5.9	9.35	10.28 ± 1.0	+ 9.95
324/200	1045-1110	10	275	8.15	8.15	$8.01 \pm .91$	- 1.72
324/300	1215-1255	12	275	6.6	8.15	$6.5 \pm .81$	-20.2
324/400	1431-1506	13	275	6.9	6.90	$5.18 \pm .90$	-24.9
324/500	1533-1606	10	275	6.75	6.80	$5.98 \pm .86$	-12.06
324/600	1621-1716	11	275	7.2	8.00	5.51 ± 1.0	-18.6
325/100	813- 842	10	445	10.2	7.75	$5.76 \pm .70$	-25.7
325/200	939-1050	11	2500	9.6	8.15	10.01 ± 2.21	+22.7
325/300	1202-1323	12	2500	9.5	8.20	10.41 ± 2.44	+26.9
329/100	933-1036	11	300	8.9	7.70	$5.1 \pm .99$	-33.7
329/200	1047-1146	12	300	7.9	8.25	6.22 ± 1.45	-24.2
329/300	1407-1454	9	300	8.8	7.60	7.23 ± 2.6	- 4.87
329/400	1533-1629	12	300	8.2	8.20	6.86 ± 1.13	-16.34
331/100	908- 952	6	1950	5.5	8.15	10.16 ± 1.10	+24.5
331/200	1000-1029	8	1950	6.1	8.15	8.7 ± 1.42	+ 6.7
331/300	1121-1215	12	1950	6.75	8.15	9.19 ± 2.14	+12.8
331/400	1215-1324	11	1950	6.75	8.15	10.73 ± 2.51	+31.7
331/500	1330-1509	7	1950	5.6	8.15	$8.71 \pm .98$	+ 6.8
401/300 + 400	1235-1306	7	5600	9.0-11.1	6.43	10.49 ± 2.18	+63.0
401/600	1425-1440	2	300	10.2	6.67	$5.75 \pm .14$	-13.8

TABLE 8.2

SUMMARY OF THE MASS FLUX COMPUTATION AND THEIR COMPARISON WITH HYDRO MASS BALANCE DATA. THE WIND SPEED USED WAS TAKEN FROM AN AVERAGE OF TETHERSONDE AND PIBAL DATA AT THE PLUME HEIGHT.

Day/line Code	Time	# of Traverses	Distance to Traverse	Hydro Mass Emissions	Calculated Mass Flux Using Tethersonde Windspeed	Calculated Mass Flux Using Windspeed From Pibal Data Averaged Over 100-500 m
			M	kg/sec	kg/sec	kg/sec
323/100	941-1008	6	300	9.15	9.20	8.71
323/300	1138-1211	9	300	9.30	12.61	7.50
323/400	1215-1240	8	300	9.35	-	8.01
324/200	1045-1110	10	275	8.15	8.10	7.96
324/300	1215-1255	12	275	8.15	6.50	-
324/400	1431-1506	13	275	6.90	5.18	-
324/500	1533-1606	10	275	6.80	6.30	5.35
324/600	1621-1716	11	275	8.00	6.90	-
325/100	813- 842	10	445	7.75	-	5.76
325/200	939-1050	11	2500	8.15	-	10.00
325/300	1202-1323	12	2500	8.20	-	10.41
329/100	933-1036	11	300	7.70	-	5.10
329/200	1047-1146	12	300	8.25	-	6.22
329/300	1407-1454	9	300	7.60	7.12	7.27
329/400	1533-1629	12	300	8.20	-	6.86
331/100	908- 952	6	1950	8.15	10.16	9.61
331/200	1000-1029	8	1950	8.15	9.62	7.84
331/300	1121-1215	12	1950	8.15	8.95	9.53
331/400	1215-1324	11	1950	8.15	10.73	-
331/500	1330-1509	7	1950	8.15	8.78	8.69
401/300 + 400	1235-1306	7	5600	6.43	-	14.23
401/600	1425-1440	2	300	6.67	-	-

TABLE 8.3 Comparison of Mass Flux Computed by Using Windspeed from Different Meteorological Systems

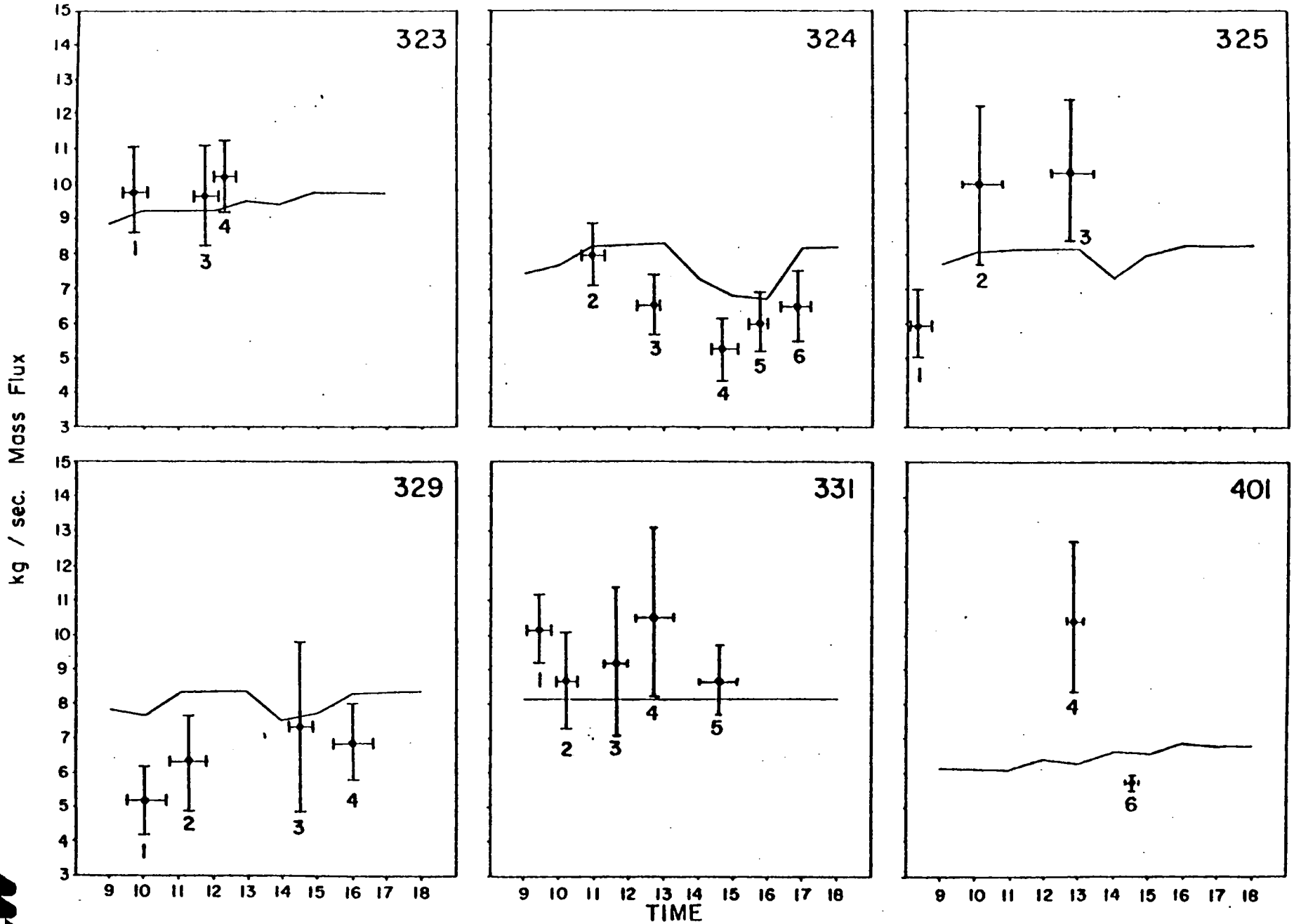

Figure 8.17 COMPARISON OF HYDRO MASS BALANCE DATA TO MASS FLUX CALCULATIONS USING METEOROLOGICAL DATA FROM AN AVERAGE OF TETHERSONDE AND PIBAL DATA

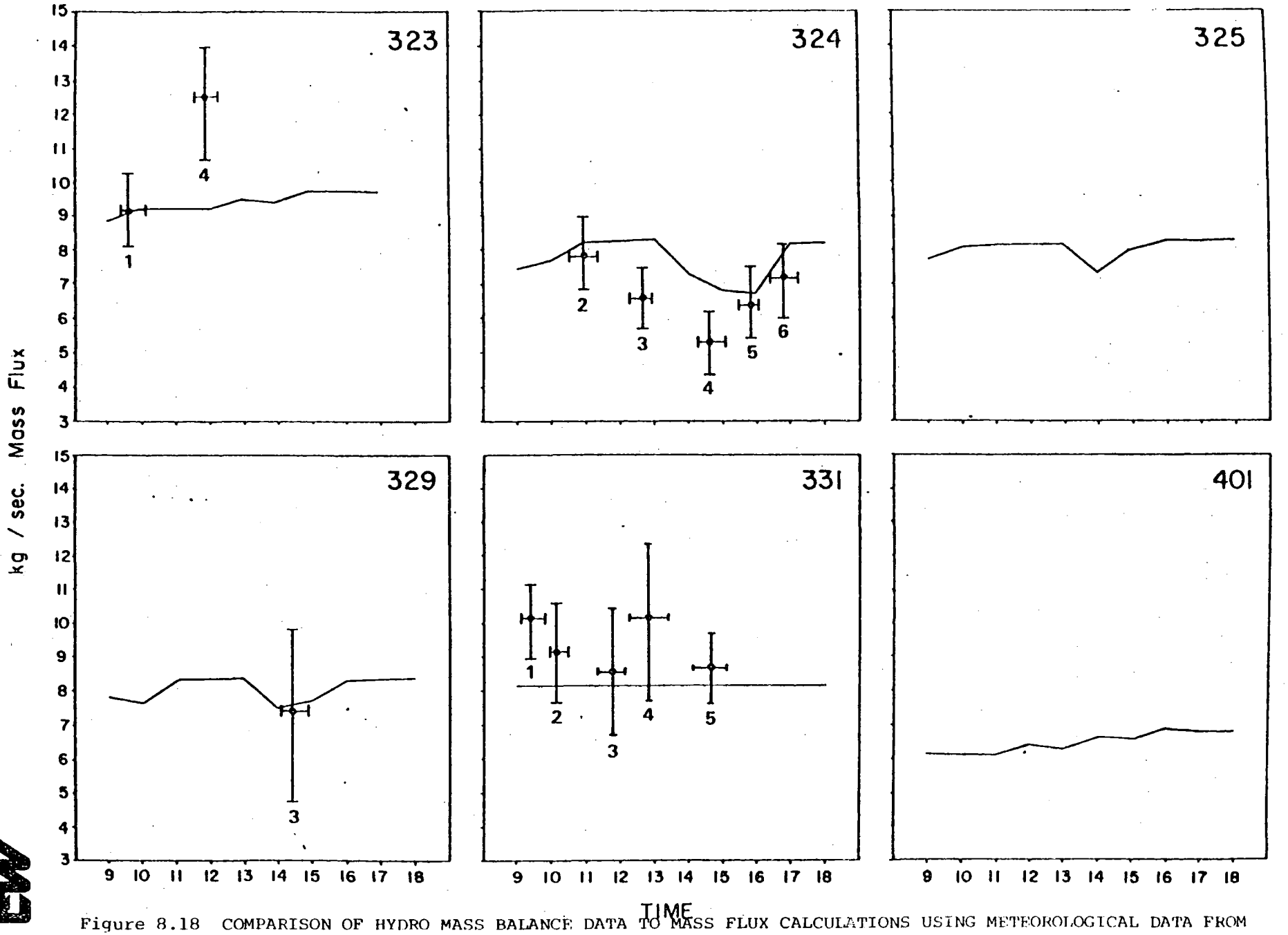

Figure 8.18 COMPARISON OF HYDRO MASS BALANCE DATA TO MASS FLUX CALCULATIONS USING METEOROLOGICAL DATA FROM TETHERSONDE

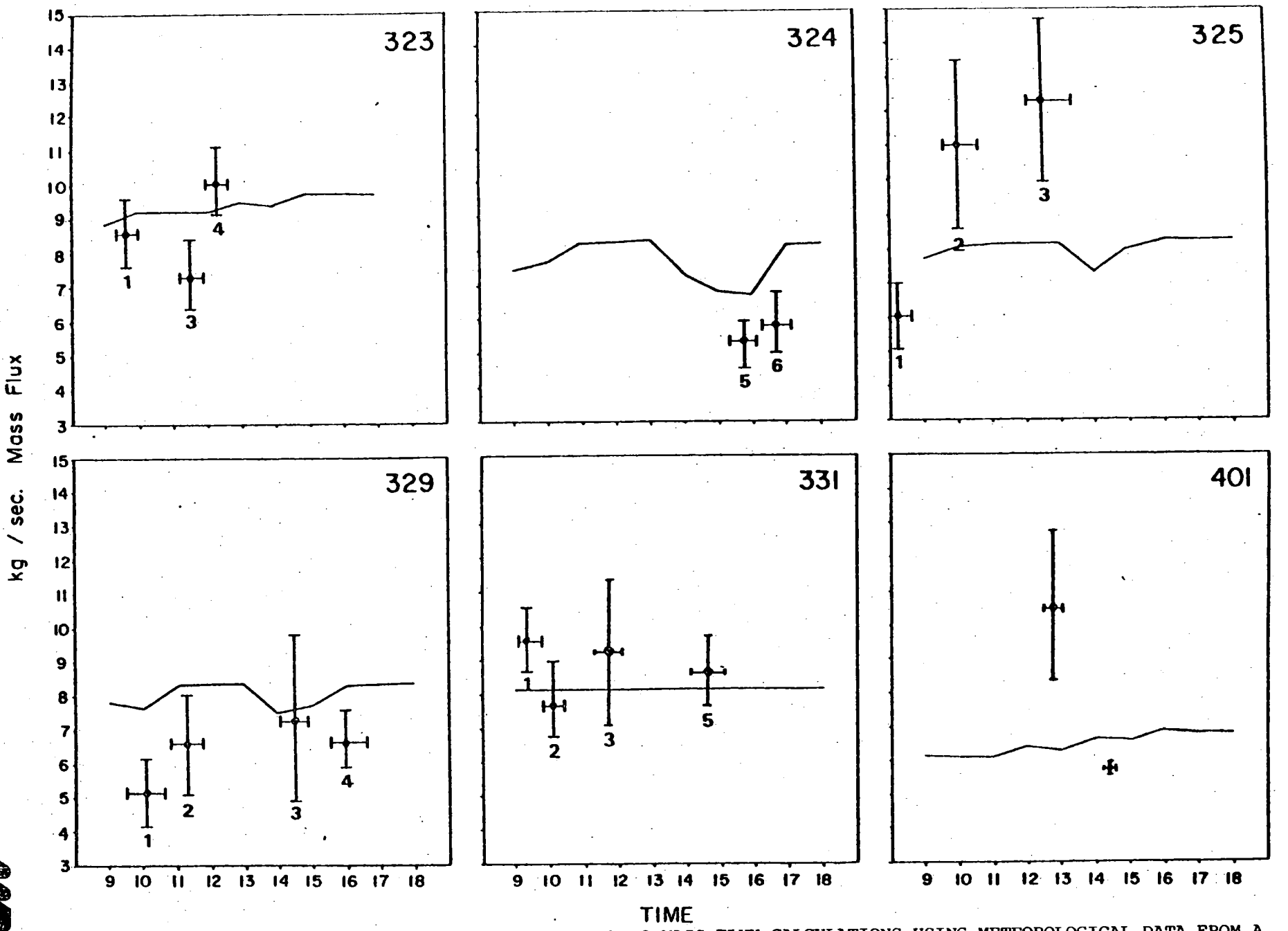

Figure 8.19 COMPARISON OF HYDRO MASS BALANCE DATA TO MASS FLUX CALCULATIONS USING METEOROLOGICAL DATA FROM A VECTOR AVERAGE OF PIBAL DATA (AVERAGED 100 - 500 m)

8.3 EVALUATION OF WIND DIRECTION MEASURFMENTS

The centre of gravity of the plume was computed alona the vehicle traverse. The direction of location of the centre of gravity was then compared with the wind direction measured with different sensors. If this angle was more than a preset value of 20 degrees, the wind direction used in the analysis was altered by an iterative method until it was within a reasonable limit of 20 degrees. Small changes in wind direction can be very crucial when the traverse is not perpendicular to the plume direction.

Table 8.1 shows the optimum plume direction obtained either from one of the meteorological sensors or from comparison of these measurements to the calculation of centre of gravity of the plume. This plume direction was compared with the wind direction measurements from pibal and tethersonde meteorological systems. It was found that in most cases, the wind direction measurements defined the plume axis quite well.

8.4 COMPUTATION OF MASS FLUX FROM INDIVIDUAL STACKS

For the correlation spectrometer data on 24th and 29th March, it was possible to resolve the response due to emission from the individual stacks. The mass emission data obtained from Hydro for each stack was then compared with these measurements.

The mass flux values were calculated for one stack (east) and subtracted from the total mass flux to determine the mass flux from the other (west). These data are summarized in Table 8.4.

Figure 8.20 and Figure 8.21 show the data obtained for the east and west stacks on 24th and 29th March respectively. The spectrometer signal returned to its background level between responses from individual stacks, during the traverse. To determine the mass flux due to

EAST STACK

Day/line	Time	Distance to Traverse m	Hydro Mass Emission kg/s	COSPEC Mass Flux kg/s	% Error	% Error for Total Mass Flux
						(Table 8.2)
324/200	1045 - 1110	275	4.11	5.67	+37	- 1.72
324/300	1215 - 1255	275	4.11	3.49	-15	-20.2
324/400	1431 - 1506	275	3.49	3.21	- 8	-24.9
324/500	1533 - 1606	275	3.54	4.16	+17.5	-12.06
324/600	1621 - 1716	275	4.03	3.63	-10	-18.6
329/100	933 - 1036	300	4.04	2.61	-35	-33.7
329/200	1047 - 1146	300	4.13	2.91	-29	-24.02
329/300	1407 - 1454	300	4.03	3.53	-12.5	- 4.87
329/400	1533 - 1629	300	4.15	3.51	-15	-16.34

WEST STACK

Day/line	Time	Distance to Traverse m	Hydro Mass Emission kg/s	COSPEC Mass Flux kg/s	% Error	% Error for Total Mass Flux
						(Table 8.2)
324/200	1045 - 1110	275	4.04	2.26	-44	- 1.72
324/300	1215 - 1255	275	4.04	2.78	-31	-20.2
324/400	1431 - 1506	275	3.41	1.85	-45	-24.9
324/500	1533 - 1606	275	3.26	2.08	-36	-12.06
324/600	1621 - 1716	275	3.97	1.94	-49	-18.6
329/100	933 - 1036	300	3.66	2.55	-30	-33.7
329/200	1047 - 1146	300	3.57	3.80	-27.	-24.02
329/300	1407 - 1454	300	3.57	3.80	+ 6.5	- 4.87
329/400	1533 - 1629	300	4.05	3.33	-17.7	-16.34

TABLE 8.4

Separate Stack Data

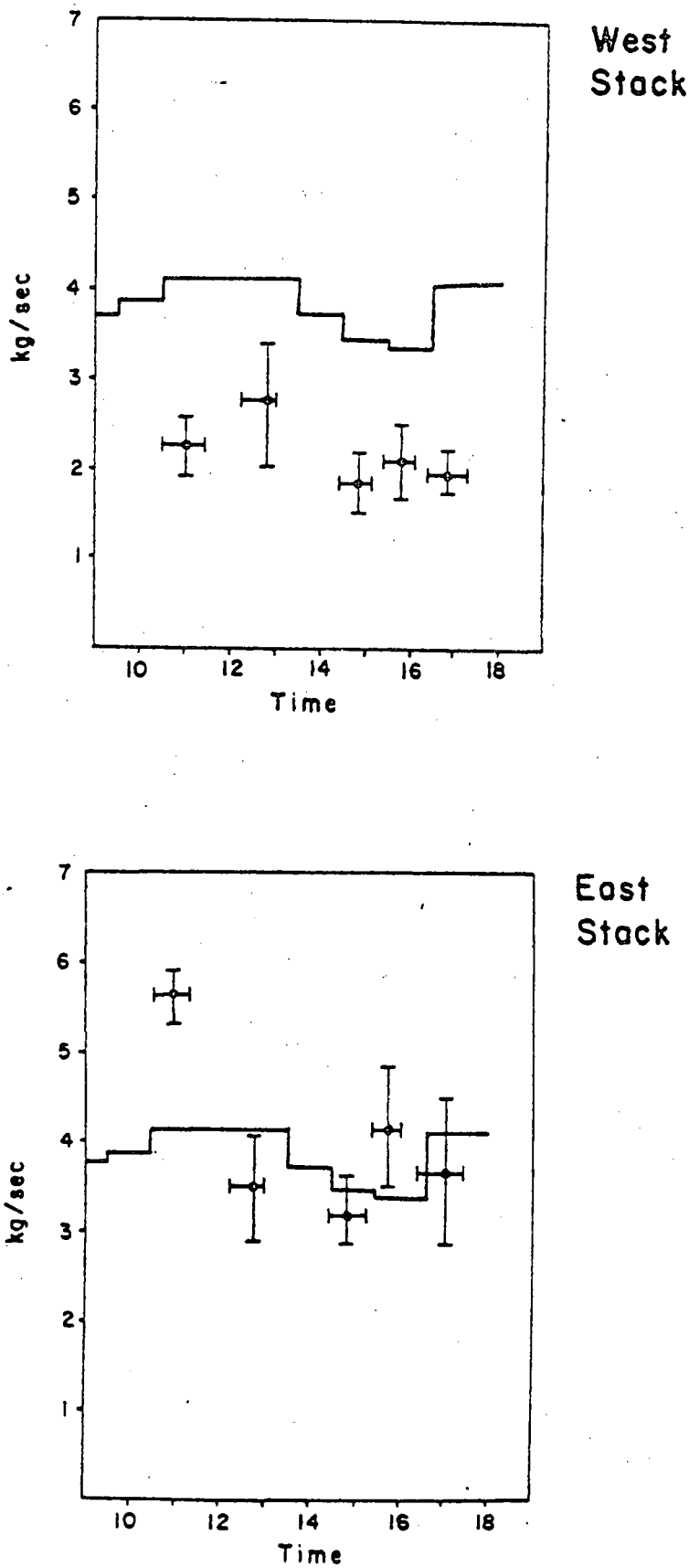

Figure 8.20 RESOLUTION OF CALCULATED MASS FLUX FROM INDIVIDUAL STACKS MARCH 24, 1978

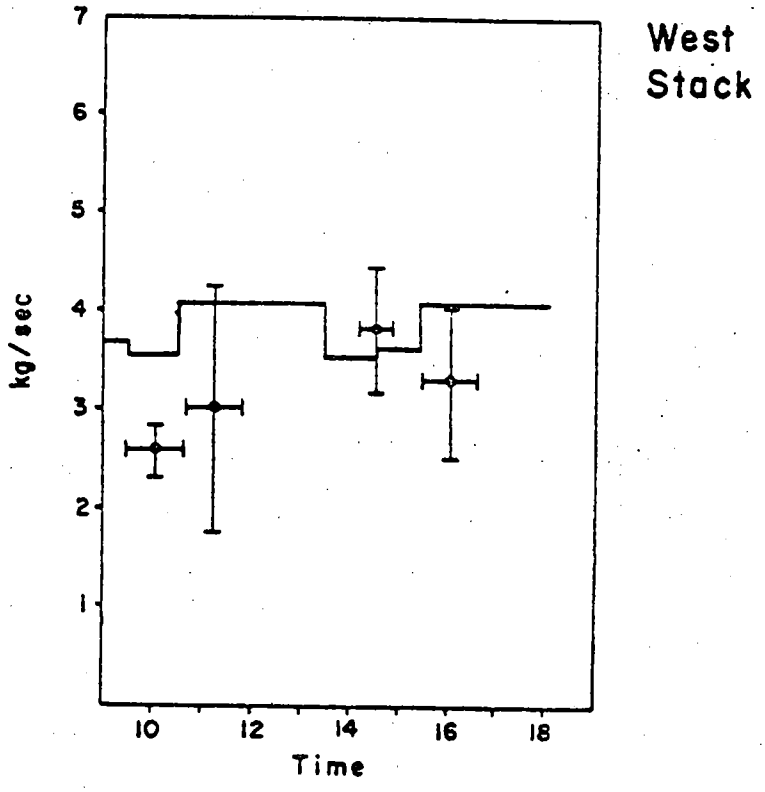

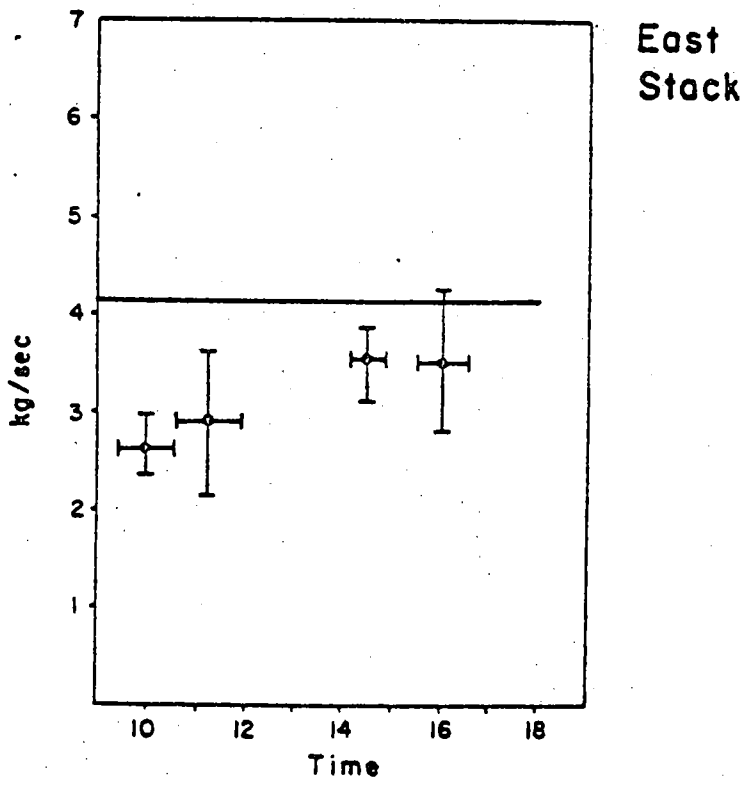

Figure 8.21 RESOLUTION OF CALCULATED MASS FLUX FROM INDIVIDUAL STACKS MARCH 29, 1978

individual stacks, the distance travelled by the vehicle was computed to the point where the instrument response due to the SO_2 in the first plume had decreased to background. This distance was used to determine various traverse segments' magnitude and direction, and analysis was carried out on the response from the individual plumes in a similar fashion.

8.5 COMPARISON WITH THE MASS BALANCE DATA AND ERROR ANALYSIS

Figures 8.17, 8.18, 8.19, 8.20 and 8.21 depict mass flux calculations from the correlation spectrometer and the corresponding mass emission data computed from mass balance of the sulphur content in the coal burnt. Table 8.2 shows these data in a tabular form. The per cent difference of the remote measurements compared to mass balance calculations was also computed. Histograms of these errors for all the data obtained in this study were plotted in figure 8.22. In figures 8.20 and 8.21, mass flux data for the individual stacks were compared with mass balance of sulphur in fuel fired in separate units.

Very good agreement was obtained between the correlation spectrometer measurements and the mass balance data for most sets of measurements. Data on 23rd March were within 10% of each other. Standard deviation of temporal variation in mass flux as measured by the correlation spectrometer was less than 15% of the mean values for the three different occasions.

In the 24th March data, variations in the mass flux were quite large from morning to evening. Correlation spectrometer data and mass balance data both show similar temporal trends. The remote sensing measurements were within 2 to 25% of mass balance data for this day. Analysis of individual stacks on this day (figure 8.20) shows that agreement on the east stack data was reasonably good while the spectrometer data from the west stack were consistently lower. This was the reason for discrepancy in total mass flux data.

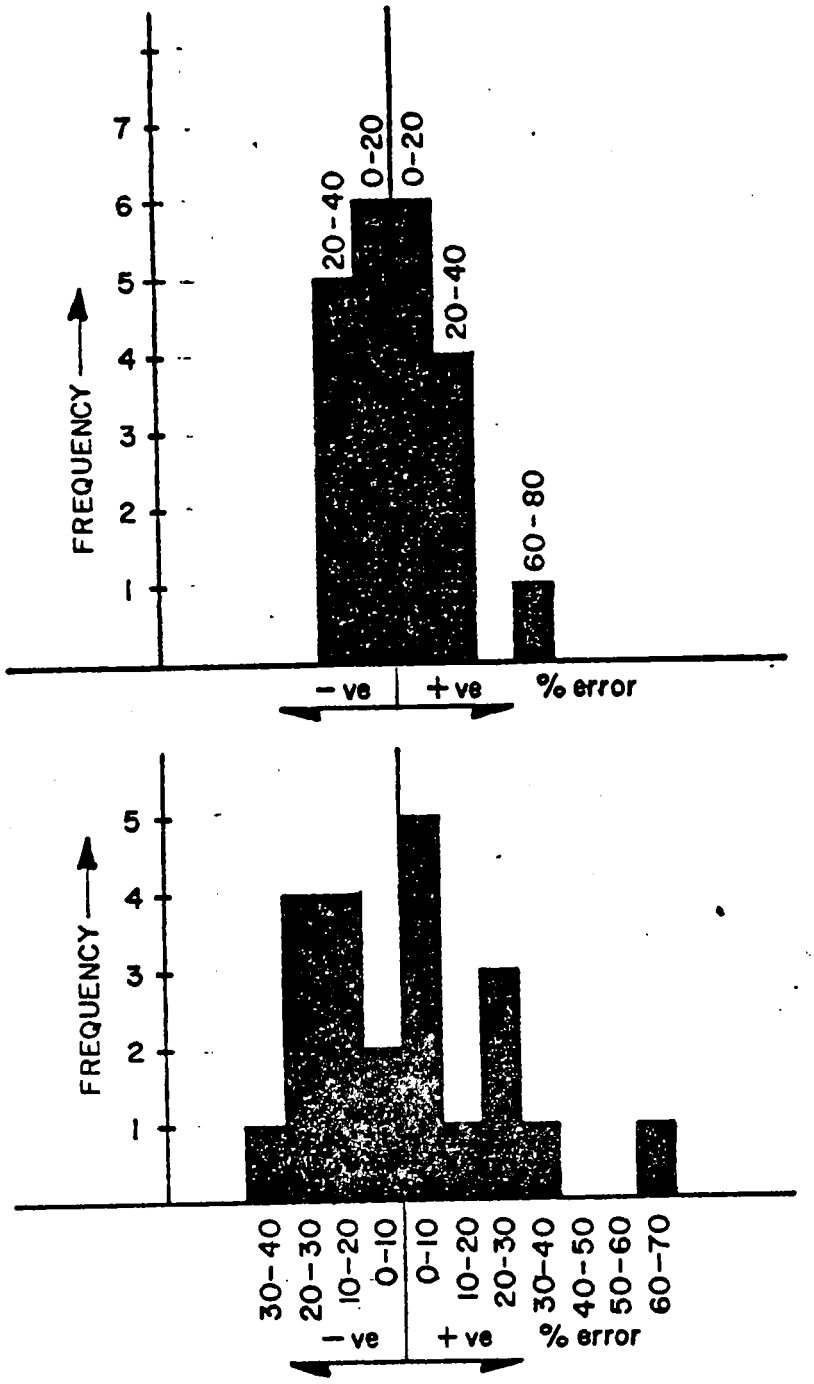

Figure 8.22 HISTOGRAMS OF DIFFERENCES BETWEEN HYDRO MASS BALANCE DATA AND CALCULATED MASS FLUX. UPPER HISTOGRAM USES SAMPLING AT 20% WHILE LOWER SAMPLES AT 10%.

The first run on 25th March was made on the road south of the Hydro stacks. On this day, the wind speeds were very high and large temporal and vertical variations were measured in the wind direction. The remote sensing data for this day were within 27% of the mass balance data.

On 29th March, the error in mass emission measurements were as high as -34% in the morning and were as low as -5% in the afternoon. The errors on 31st March data taken at a road north of the stacks were within 6 to 32%.

On 1st April, it was difficult to traverse under the complete plume for most of the day by using local roads. The wind direction was varying rapidly and it was possible to traverse under the complete plume only on the two occasions recorded in Table 8.2. It was shown that while data for the line 401/600 taken close to the stacks were within about 14%, the error for data recorded on the east side of the plant (near Peacock Point at about 6 km) was 64%. This large error was suspected to be due to a change in the wind field from the stacks to Peacock Point. For more reliable data, it would have been advantageous if wind measurements closer to the location of the correlation spectrometer had been available and the measurement statistics had been improved by making a larger number of traverses.

From histograms in figure 8.22, it was computed that the average mean of error for all the data is +0.98%. The standard error was computed to be 23.56%. Therefore, on the basis of the data presented in this report, it may be concluded that there was a 70% probability for the correlation spectrometer data to provide mass emission results within 25% of mass balance values. When the measurements made at Peacock Point were neglected, the mean error was -1.97%, and the standard error, 19.5%; i. e., within a perimeter of 2.5 km around the plant, there was, therefore, a 70% probability that the correlation spectro-

meter data were within 20% of the mass balance; or an 86% probability that all measured data were within 25% of the mass balance. It should, however, be noted that only the mean value of the mass flux from the correlation spectrometer data has been used in this analysis. The correlation spectrometer has yielded measurements much closer to the mass balance data on certain specific runs. In this study, we attempted to obtain a large amount of data to statistically evaluate the remote sensing measurement. It was apparent that a much larger data bank would be required to fine tune the confidence levels and limitations of this technique, to better define the reliability and accuracy of the method, and to extend this methodology to medium and long range transport studies. It should be emphasized that the comparison of the measurements made during this study has been carried out against the mass balance method used by Ontario Hydro scientists. The stacks at the Nanticoke plant were not instrumented for environmental monitoring. Therefore, the hourly average of power generated, the fuel consumption at that load, and sulphur content in coal obtained from a weekly chemical analysis were used to predict emission rates of the SO_2. These data, therefore, do not provide information on any transient temporal variations.

Further, sulphur content in the fuel was taken as 2.42% for the data taken from 23rd March, 1978 to 29th March, 1978, and it was measured to be 2.3% in the week beginning on 30th March.

By using a weekly value, the mass emission predictions can be be in error up to 5%. Historical data on sulphur content show that variation in the weekly measurement of sulphur content can be different by more than 15% on two consecutive weeks. Such uncertainties make it difficult for the mass balance technique to be free from errors due to the inherent assumptions. The error analysis presented above assumes that the effect of these assumptions is negligible; i. e., 1) the temporal variation in sulphur content of coal is negligible and equal to laboratory measurements during the week, 2) there is complete combustion and

conversion of sulphur into SO_2, and 3) the average value determined from remote sensing data correspond directly with the average hourly values of mass balance data.

Table 8.5 is a summary of the total collected data showing the measurement distance from the source, the number of traverses during a single sample period, the measured wind speed and the relative accuracy of the mass flux measurements. Neglecting the Peacock Point data, 5.6 km from the source, where insufficient sampling periods were performed to draw statistical conclusions, there does not appear to be any direct relationship between the relative errors and the distance from the source, the number of traverses or the wind speed.

8.6 DISCUSSION OF INFRARED GAS CELL SPECTROMETER DATA

Several instrumental limitations became evident during the program:

1) Effects of changing background radiance in sensor field of view. Unfortunately, while the criticality of the instrument optical alignment is well known, its optical balance condition was not verified in the laboratory prior to the field program. The instrument operation in the field in the presence of changing background radiation clearly demonstrated that severe optical imbalance between the signal and reference arms did exist. In the presence of a uniform background, clear sky or overcast sky, the effect was not present. The alignment equipment necessary and the time required did not make it possible to improve this condition in the field. On the occasions when the instrument was operated at night in the presence of intermittent cloud cover, no meaningful data were collected due to this instrumental effect.

2) Polarization effects: On the large number of occasions when uniform background radiation were present, data was collected with the gas cell spectrometer, and instrument responses due to the presence of the plume in the field of view were obtained. These responses were obtained while working close to the source ($\sim$ 500m) and carrying out lines from east to west. However, under these optimum background conditions, when the instrument was rotated through 180° to carry out the

Day/line	# of Traverses	Wind Speed m/s	Distance from Source m	% Error
South Road				
323/100	6	5.6	300	+ 8.2
323/300	9	6.0	300	+ 4.84
323/400	8	5.9	300	+ 9.95
324/200	10	8.15	275	- 1.72
324/300	12	6.6	275	-20.2
324/400	13	6.9	275	-24.9
324/500	10	6.75	275	-12.06
324/600	11	7.2	275	-18.6
325/100	10	10.2	445	-25.7
329/100	11	8.9	300	-33.7
329/200	12	7.9	300	-24.2
329/300	9	8.8	300	- 4.87
329/400	12	8.2	300	-16.4
401/600	2	10.2	300	-13.8
Stelco				
325/ 200	11	9.60	2500	+22.7
325/300	12	9.50	2500	+26.9
North Road				
331/100	6	5.5	1950	+24.5
331/200	8	6.1	1950	+ 6.7
331/300	12	6.75	1950	+12.8
331/400	11	6.75	1950	+31.7
331/500	7	5.6	1950	+ 6.8
Peacock Pt.				
401/400 + 300	6	9-11	5600	+63.0

TABLE 8.5 Summary of Related Parameters

return traverse, west to east, a large offset ($\sim$500 ppm-m SO_2) appeared on the instrument output, resulting in an imbalance condition and no appreciable signal due to the presence of the plume at this orientation was then detected. These data strongly suggest that the instrument is extremely sensitive to polarization effects, brought about when the field of view changes location on the sky with respect to the solar location. Polarization effects are well known in the UV and while they are known to exist in the IR, little quantitative work has been carried out to evaluate their extent. These effects will also obviously be present when the instrument is used in absorption using the ground as the background source, even though they will be reduced in magnitude by reflection from the ground. However, where one is attempting to make highly sensitive measurements to the level of $1:10^4$ of background signal, they would be quite severe. Due to these operational limitations, no meaningful burden data could be extracted from the instrument responses.

APPENDIX

Summary

Dispersive correlation spectroscopy was first used to study water vapour in planetary atmospheres (Botema et al, 1964) and subsequently to measure trace amounts of sulphur dioxide (Kay, 1967). The early development of the technique and its application to pollution studies led to a series of mask correlation spectrometers under the trade name COSPEC. (Newcomb and Millan, 1970; Moffat et al., 1971; Moffat and Millan, 1971). More recently, similar instruments have been developed (Bonafe et al, 1976; Brewer, 1973), similar in concept but differing in implementation.

Although almost all the work to date has been carried out with dispersive spectrometers, several non-dispersive spectrometers have also been developed (Laurent, 1975; Ward and Zwick, 1975; Bartle, 1974). Their sensitivity and performance characteristics are very similar to those of the COSPEC; however, they suffer from a lack of in-depth field evaluation.

Operating Configurations

Several papers have appeared on the use of correlation spectrometers in conjunction with lamps to measure pollutants over paths of up to 8 km (Newcomb and Millan, 1970; Moffat et al, 1971; Bonafe et al, 1976, Sandroni and Gerutti,1977). These measurements offer several advantages over those made by point monitors: 1) operation over suitable paths yields data better suited to regional studies; 2) the method is very sensitive (better than 1 ppb); and 3) the measurements are made without contact. Despite these advantages, the method has so far been used only in relatively short term studies.

Passive Measurements

Remote sensors have been widely used in the passive mode to measure burdens (concentration x path length), primarily of sulphur dioxide, along the path of scattered radiation. In particular, many surveys have been conducted with instruments looking vertically upwards from ground-based vehicles, either upwards or downwards from aircraft and through slant paths at the plume close to the stack exit.

The first measurements of the emission from a particular source were made from fixed locations by observing the plume just above the chimney top (Moffat and Millan, 1971). However, this procedure depends on the geometry and velocity of the plume in a region where they are difficult to define. Some more recent measurements in this mode (Barnes et al, 1974) show that agreement with in-stack readings at the closest range is quite good. However, at greater distances, correlation becomes poor. They conclude that the main limitation is inadequate compensation for scattering both in the plume and in the intervening atmosphere. (Bartle et al, 1974) reports measurements made in the slant path with a non-dispersive spectrometer, the results of which compared more favourably with in-situ extractive and Method 6 techniques. Agreement was claimed to be within the experimental error between the methods.

The more usual operating mode is to traverse beneath the plume looking vertically upwards at distances varying up to 10 km from the source (Jepson and Langan, 1974; Ward, 1977; Jain and Ward, 1978; Sullivan et al, 1977). The flux is then found by measuring burdens in the plume relative to background values outside it, integrating with distance across wind, and multiplying by a suitable wind speed. Several traverses are normally needed, because of random variations introduced by fluctuations in wind speed and direction. In a study of this method, based on 465 traverses, Sperling (1975), found that an accuracy of $\pm$ 30% (standard deviation) could be achieved over a 20-minute period with an average of five traverses. Most of the inaccuracy was reported to be associated with the wind speed.

A further limitation is that measured burdens refer to some "effective" path. In an ideal situation, the pollutant lies in a clear particle-free atmosphere and is illuminated entirely from behind. In practice, the plume will contain particles which scatter radiation into the line of sight from other angles. If the gas is distributed uniformly in horizontal layers, this can only increase the effective path length and inflate measurements of vertical burden. For an isolated plume, however, the measurements could be either increased or reduced (Moffat and Millan, 1971). If the concentration of particles is high, multiple scattering within the plume or layer could further increase the effective path. During a recent survey, two or more spectrometers simultaneously observed enhanced burdens in a power station plume on several occasions (Moore and Hamilton, 1977). The values were as much as two or three times those calculated from source emission and wind data. They were most marked when the plume became mixed with a layer of low cloud or when it contained clearly visible quantities of condensed water vapour. Preliminary results from a theoretical study of the problem (Millan, 1978), indicate that such enhancements can easily occur in plumes, but that measurements in a mixing layer with depth 1 km and visibility 5 km would not be enhanced by more than about 10% (Sutton and Varey, 1977).

Since correlation spectrometers measure vertical integrals, they are invaluable for detecting the plumes emitted from tall chimneys and studying their horizontal dispersion. (Millan et al, 1976; Millan, 1976) have discussed the relevant procedures as they applied them to a study of the plume from a 380m stack at Sudbury, Ontario. They have shown the value of interpreting cross wind profiles in terms of both Eulerian averages (in a fixed coordinate frame) and Lagrangian averages (relative to the plume axis). The latter are particularly useful for studying the effects of wind shear and bifurcation (Fanaki, 1975). The study of some aspects of dispersion, such as its dependence on distance of travel, can only be carried out effectively by deploying several units

simultaneously. Up to five teams cooperated in this way on campaigns organized recently by the Commission of the European Communities at Lacq (1975) and Drax (1976) (Guillot, 1977, Remote Sensing, New Orleans).

In recent years, much attention has been directed towards the transformation and deposition of sulphur dioxide during its transport over distances of the order of 1,000 km. Since correlation spectrometer can measure fluxes, they have been used to determine depletion rates (Gillani and Husar, 1976 ; Fisher et al, 1977; Ward and Jain, 1977). However, due to the errors introduced by uncertainties in emission, the sampling period required to develop sufficient statistics and errors in wind speed, the overall accuracy is low. This accuracy should be improved with simultaneous sampling at different distances.

Despite some quantitative limitations which, when carefully interpreted, can, in many instances, be overcome, correlation spectrometers have emerged as almost indispensable tools for the efficient conduct of mobile surveys. It is a very sensitive instrument capable of locating plumes 100 km or more from their source (Williams, 1976; Millan and Chung, 1977). It has also proved invaluable in supplementing measurements from fixed networks of ambient monitors (Davies et al, 1975; Van Egmond, 1976).

REFERENCES

1. Barnes, H. M., Herget, W. F., and Rollins, R., Remote sensing of SO_2 in power plant plumes using ultraviolet absorption and infrared emission spectroscopy, in Analyt. Methods Appl. to Air Pollution Measurements, ed. R. K. Stevens, W. F. Herget, Ann Arbor Sci. Publ. Inc. (1974).

2. Barringer, A. R., and Newbury, B. C., Molecular corr. spec. for sensing gaseous pollutants, paper 67/196, 60th Ann. APCA mtg. (1967).

3. Bartle, E. R. (1974), EPA contract # 68-02-1481, Final Rpt.

4. Bonafe, M. et al (1976), Mask correlation spectrophotometry: advanced methodology for atmospheric measurements, AE 10, 469-474.

5. Botema, M. (1964), Plummer, W. and Strong, J., Water vapour in the atmosphere of Venus, Astrophys. J. 139, 1021-1022.

6. Brewer (1973), A replacement for the Dobson spectrophotometer, Pure and Appl. Geophys., Vol. 106-108, 919-920.

7. Davies, J. H. et al (1975), Detection of a plume 400 km from the source, AE 11, 939-944.

8. Fanaki, F. H. (1975) Experimental observations of a bifurcated buoyant plume, boundary layer, Meteorology 9, 490-495.

9. Fisher, B. E. A. et al (1977), Observations and calculations of airborne sulphur from multiple sources out to 1000 km, AE 11, 1163-1170.

10. Gillani, N. W. and Husar, R. B. (1976), Mathematical modelling of air pollution - a parametric study, Proc. of second fed. conf. on the Great Lakes.

11. Guillot, P. (1977), Joint EC campaign on remote sensing of SO_2 pollution from a gas plant in Lacq (France), Proc. of 4th joint conf. on sensing of environmental pollutants, New Orleans, La.

12. Hoff, R. M., Gallant, A. J., and Millan, M. M., COSPEC data processing procedures, report from AES, Downsview, Ont. (1977).

13. Jepson, A. F. and Langan, L. (1974), Gas flow measurement by plume analysis, Flow, Vol. 1, Pt. 1, 361-367, Instrument Soc. of America, Pittsburg, Pa.

14. Kay, R. B., Absorption spectra apparatus using optical correlation for the detection of trace amounts of SO_2, Appl. Optics 6, 776 (1967).

15. Laurent, J. (1975) Selective modulation radiometer, ONERA, Chatillon, France, unpublished.

16. Millan, M. M. (1978), private communication.

17. Millan, M. M., A note on the geometry of plume diffusion measurements, Vol. 10, Pergamon Press (1976).

18. Millan, M. M., Hoff, R. M., Gallant, A. J., Tall stacks, plume dispersion, and emission calculations by corr. spectroscopy, presented at the 69th Annual Mtg. of the APCA, Portland, Ore., June, 1976.

19. Millan, M. M., Townsend, S. J., and Davies, J. A., Study of the Barringer refractor plate corr. spec. as a remote sensing instrument, U. of T, Dept. 149 (1970).

20. Millan, M. M., Gallant, A. J. and Turner, H. E. (1976), The application of corr. spectroscopy to the study of dispersion from tall stacks, AE 10, 499-511.

21. Moffat, A. J., and Millan, M. M., The application of optical correlation techniques to the remote sensing of SO_2 plumes using skylight, AE 5, 677 (1971).

22. Moffat, A. J., Robbins, J. R. and Barringer, A. R. (1971), Electro-optical sensing of environmental pollutants, AE 5, 511-525.

23. Moore, D. J., and Hamilton, P. M. (1977), Report on 2nd CEC campaign of remote sensing of air pollution at Drax, CERL, Leatherhead, England (unpublished).

24. Newcomb, G. S. and Millan, M. M. (1970),Theory, applications and results of the long line corr. spec. IEEE Trans. Geosci. Electron. GE-8, 149-157.

25. Ryan, J. R. and Booth, M. R., Nanticoke GS air quality monitoring program and 1976 results, Ont. Hydro Env. Prot. Dept. Rpt., CTS-07012-6 (1977).

26. Ryan, J. R. (1978) official communications.

27. Sandroni, S. and Gerutti, C. (1977), Long path measurements of atmospheric sulphur dioxide, AE 11, 1225-1232.

28. Sperling, R. B. (1975), Evaluation of the corr. spec. as an area SO_2 monitor, NTIS, Springfield, Va., EPA-600/2-75-077.

29. Sullivan, J. L., Simmons, A., and Lim, B. S., Remote sensing by a Barringer COSPEC of sulphur dioxide emissions from Nanticoke Elec. Gen. Stn., U. of W. O. rpt. to Ont. Hydro (1977).

30. Turner, D. B. (1969), Workbook of atmos. dispersion estimates, U.S. Dept. of H, E and W, Public Health Service Publ. No. 999-AP-26. Available from Natl. Air Plll. Con. Adm., U.S. Dept. of H,E and W, Cincinnati, Ohio.

31. Van Egmond, N. D. (1976) private communications.

32. Ward, T. V. and Jain, S. C., Remote sensing study to determine the downwind deposition of SO_2 from the INCO smelter, MONITEQ rpt. prepared for ARB, OME (1978).

33. Ward, T. V., and Zwick, H. H., Gas cell corr. spec., Appl. Optics 14, 2896 (1975).

34. Williams, D. (1976), private communications.

35. Ward, T. V. (1977), Data and results from a ground mobile corr. spec. study of emissions from a smelter, MONITEQ Tech. Rpt. MTR77-1.